

1 **Supporting Information**

2

3

4 **Stability of Per- and Polyfluoroalkyl Substances in Solvents Relevant to**
5 **Environmental and Toxicological Analysis**

6

7 Chuhui Zhang,¹ Amie C. McElroy,¹ Hannah K. Liberatore,² Nancy Lee M. Alexander,¹ and
8 Detlef R.U. Knappe^{1,3*}

9

10 ¹Department of Civil, Construction, and Environmental Engineering, North Carolina State
11 University, Raleigh, North Carolina 27695, United States

12 ²Center for Environmental Measurement and Modeling, Office of Research and Development,
13 U.S. Environmental Protection Agency, Research Triangle Park, North Carolina 27711, United
14 States

15 ³Center for Human Health and the Environment, North Carolina State University, Raleigh, North
16 Carolina 27695, United States

17

18

19 *Corresponding Author E-mail: knappe@ncsu.edu

20

21

22

23	Table of Contents	
24	Text S1. Liquid chromatography-mass spectrometry (LC-MS) analysis	5
25	Text S2. PFAS quantitation for LC-MS analysis.....	5
26	Text S3. Quality assurance/quality control (QA/QC) for LC-MS analysis	6
27	Text S4. Headspace gas chromatography-mass spectrometry (GC-MS) method for Fluoroethers E-1, E-2,	
28	and E-3	6
29	Text S5. Gas chromatography-high resolution mass spectrometry (GC-HRMS) analysis for degradation	
30	product identification	8
31	Text S6. First-order kinetics	9
32	Text S7. Arrhenius equation	10
33	Text S8. Calculation of molar yield.....	10
34	Table S1. Per- and polyfluoroalkyl substances (PFASs) targeted in this study	11
35	Table S2. Structures of 1,2,2,2-Tetrafluoroethyl trifluoromethyl ether and Fluoroethers E-1, E-2, and E-3	
36	13
37	Table S3. Stability of PFASs in deionized water at room temperature (20.2°C) for 7 and 30 days	14
38	Table S4. Stability of PFASs in methanol at room temperature (20.2°C) for 7 and 30 days	15
39	Table S5. Stability of PFASs in isopropyl alcohol (IPA) at room temperature (20.2°C) for 7 and 30 days	
40	16
41	Table S6. Stability of PFASs in acetonitrile (ACN) at room temperature (20.2°C) for 7 and 30 days	17
42	Table S7. Stability of PFASs in acetone at room temperature (20.2°C) for 7 and 30 days	18
43	Table S8. Stability of PFASs in dimethyl sulfoxide (DMSO) at room temperature (20.2°C) for 7 and 30	
44	days	19
45	Table S9. Summary of the stability of PFASs targeted in this study	20
46	Table S10. First-order rate constants (<i>k</i>) of PMPA, PEPA, and HFPO-DA in acetonitrile (ACN), acetone,	
47	and dimethyl sulfoxide (DMSO) with different water-to-organic solvent ratios (100% organic solvent,	
48	90:10% (v/v) and 80:20% (v/v) organic solvent:water) at room temperature (20.2°C)	21
49	Table S11. First-order rate constants (<i>k</i>) of PMPA, PEPA, and HFPO-DA in acetonitrile (ACN), acetone,	
50	and dimethyl sulfoxide (DMSO) at three temperatures [cold (3.4°C), room (20.2°C), and hot (32.4°C)].	22
51	Table S12. Activation energy (<i>E_a</i>) and pre-exponential factor (<i>A</i>) of PMPA, PEPA, and HFPO-DA in	
52	acetonitrile (ACN), acetone, and dimethyl sulfoxide (DMSO)	23
53	Table S13. Molar yield of Fluoroethers E-1, E-2, and E-3 from the degradation of HFPO-DA, HFPO-TA,	
54	and HFPO-TeA, respectively, in acetonitrile (ACN), acetone, and dimethyl sulfoxide (DMSO) at room	
55	temperature (20.2°C) in 5 days	23
56	Table S14. The percent abundance of [M-F+1] ⁺ ion for Fluoroethers E-1, E-2, and E-3 from the	
57	degradation of HFPO-DA, HFPO-TA, and HFPO-TeA, respectively, in fully deuterated acetone	24
58	Figure S1. Molecular structures of per- and polyfluoroalkyl substances (PFASs) evaluated in this study.	26

59	Figure S2. Representative calibration curves for (A) PFHxA and (B) PFO2HxA using LC-HRMS.	27
60	Figure S3. Stability of (a) PMPA, (b) PEPA, (c) GenX, (d) HFPO-TA, (e) HFPO-TeA, (f) PFO2HxA, (g)	
61	PFO3OA, and (h) PFO5DoA in water, methanol, isopropyl alcohol (IPA), dimethyl sulfoxide (DMSO),	
62	acetonitrile (ACN), and acetone at room temperature (20.2°C).	29
63	Figure S4. Stability of perfluoroalkyl ether carboxylic acids (PFECAs): (a) mono-ether PFECAs, (b)	
64	HFPO homologues, and (c) multi-ether PFECAs in acetone at room temperature (20.2°C).....	30
65	Figure S5. Stability of perfluoroalkyl ether carboxylic acids (PFECAs): (a) mono-ether PFECAs, (b)	
66	HFPO homologues, and (c) multi-ether PFECAs in dimethyl sulfoxide (DMSO) at room temperature	
67	(20.2°C).....	31
68	Figure S6. Stability of HFPO-DA starting at different initial concentrations (10, 50 and 100 µg/L) in (a)	
69	acetonitrile (ACN), (b) acetone, and (c) dimethyl sulfoxide (DMSO) at room temperature (20.2°C).	32
70	Figure S7. Stability of PMPA in (a) acetonitrile (ACN), (b) acetone, and (c) dimethyl sulfoxide (DMSO)	
71	with different water-to-organic solvent ratios at room temperature (20.2°C).....	33
72	Figure S8. Stability of PEPA in (a) acetonitrile (ACN), (b) acetone, and (c) dimethyl sulfoxide (DMSO)	
73	with different water-to-organic solvent ratios at room temperature (20.2°C).....	34
74	Figure S9. Stability of multi-ether PFECAs in (a) acetonitrile (ACN), (b) acetone, and (c) dimethyl	
75	sulfoxide (DMSO) with different water-to-organic solvent ratios at room temperature (20.2°C).....	35
76	Figure S10. Arrhenius plots describing the temperature-dependence of first-order rate constants of HFPO-	
77	DA, PEPA, and PMPA degradation in (a) acetone and (b) dimethyl sulfoxide (DMSO).	36
78	Figure S11. Arrhenius plots describing the temperature-dependence of first-order rate constants of (a)	
79	PMPA and (b) PEPA degradation in acetonitrile (ACN), acetone, and dimethyl sulfoxide (DMSO).	36
80	Figure S12. (A) GC–Orbitrap total ion chromatogram (TIC) comparison of Fluoroether E-1 standard (top)	
81	and degradation product of HFPO-DA in acetone in 5 days in black color and acetone blank in gray color	
82	(bottom); (B) mass spectra of Fluoroether E-1 standard (top) and degradation product of HFPO-DA in	
83	acetone in 5 days (bottom); (C) mass spectra list of Fluoroether E-1 standard (top) and degradation	
84	product of HFPO-DA in acetone in 5 days (bottom).	37
85	Figure S13. (A) GC–Orbitrap total ion chromatogram (TIC) comparison of Fluoroether E-2 standard (top)	
86	and degradation product of HFPO-TA in acetone in 5 days in black color and acetone blank in gray color	
87	(bottom); (B) mass spectra of Fluoroether E-2 standard (top) and degradation product of HFPO-TA in	
88	acetone in 5 days (bottom); (C) mass spectra list of Fluoroether E-2 standard (top) and degradation	
89	product of HFPO-TA in acetone in 5 days (bottom).....	38
90	Figure S14. (A) GC–Orbitrap total ion chromatogram (TIC) comparison of Fluoroether E-3 standard (top)	
91	and degradation product of HFPO-TeA in acetone in 5 days in black color and acetone blank in gray color	
92	(bottom); (B) mass spectra of Fluoroether E-3 standard (top) and degradation product of HFPO-TeA in	
93	acetone in 5 days (bottom); (C) mass spectra list of Fluoroether E-3 standard (top) and degradation	
94	product of HFPO-TeA in acetone in 5 days (bottom).....	39
95	Figure S15. (A) GC–Orbitrap total ion chromatogram (TIC) comparison of degradation product of PMPA	
96	in acetonitrile in 5 days (top) and degradation product of PMPA in DMSO in 5 days (bottom); (B) mass	
97	spectra of degradation product of PMPA in acetonitrile in 5 days (top) and degradation product of PMPA	
98	in DMSO in 5 days (bottom); (C) mass spectra list of degradation product of PMPA in acetonitrile in 5	
99	days (top) and degradation product of PMPA in DMSO in 5 days (bottom).....	40

100 Figure S16. (A) GC–Orbitrap total ion chromatogram (TIC) of degradation product of PEPA in acetone
101 in 5 days in black color and acetone blank in gray color; (B) mass spectra of degradation product of PEPA
102 in acetone in 5 days; (C) mass spectra list of degradation product of PEPA in acetone in 5 days. 41
103 Figure S17. Proposed mechanisms of HFPO-DA degradation of Fluoroether E-1 in deuterated acetone. 44
104 References..... 45
105
106

107 **Text S1. Liquid chromatography-mass spectrometry (LC-MS) analysis**

108 LC-MS analysis was performed using an Agilent 1290 Infinity II high-performance liquid
109 chromatograph (HPLC) coupled to an Agilent 6545 quadrupole time-of-flight (QTOF) mass
110 spectrometer. Chromatographic separation was accomplished using a Zorbax Eclipse Plus C18
111 column (4.6 × 50 mm, 3.5 μm; Agilent). The method conditions were as follows: 0.4 mL/min flow
112 rate; column temperature at 50°C; 100 μL of injection volume; mobile phase A: ammonium acetate
113 buffer (5 mM) in water, and mobile phase B: methanol; gradient: 0-8 min linear from 90:10 A/B
114 to 5:95 A/B, 8-20 min 5:95 A/B; followed by a 5 min post time for equilibration. Compounds were
115 ionized by operating electrospray ionization (ESI) in negative mode. The dual-electrospray source
116 provided purine and hexakis(1H, 1H, 3H-tetrafluoropropoxy)phosphazine as internal reference
117 masses. The instrument was operated in 2GHz extended dynamic range mode with an MS mass
118 range of 70-1200 m/z. Raw data were processed using Agilent MassHunter.

119 To probe suspect features that may represent reaction products, we looked for integrated peak
120 heights that exhibited a 2-fold or greater change between samples collected at the first time point
121 and the last time point of an experiment. MS spectra collected for each feature of interest were
122 manually checked to identify reaction products, and molecular features identified in the blank were
123 removed from the sample data. Emphasis was placed on chemicals demonstrating a negative mass
124 defect, as described elsewhere.¹ Apart from the dosed PFASs, no additional fluorinated compounds
125 were observed in any of the tested solvents based on the collected LC-QTOF-MS data.

126

127 **Text S2. PFAS quantitation for LC-MS analysis**

128 Using LC-QTOF-MS data, PFAS quantitation was carried out in a fashion previously described.^{2,3}
129 PFAS concentrations were calculated from area ratios (i.e. peak area for the analytical standard
130 divided by the peak area for the isotopically labeled internal standard) and standard curves. Each
131 standard curve included seven calibration points ranging from 10 ng/L to 1,500 ng/L. Calibration
132 standards were analyzed in duplicate, once at the beginning and once at the end of each sample
133 batch. To generate standard curves, area ratios were plotted against known concentrations of the
134 calibration standards. Standard curves were mathematically described by a concentration weighted
135 (1/x), second-order polynomial fit.

136 The R² for perfluoroalkyl acids (PFAAs) was >0.99 and for per- and polyfluoroalkyl ether acids
137 (PFEAs) > 0.98. At the selected ionization conditions, variability in PFEA responses exceeded

138 those of perfluorocarboxylic acids (PFCAs) and perfluorosulfonic acids (PFSAs). Example
139 standard curves are shown in Figure S2. The quantitation limit (QL) was defined as the first point
140 of the standard curve, at which area ratios yielded calculated concentration values within $\pm 30\%$
141 error. The QL for LC-QTOF MS was 50 ng/L for PFMOAA and HFPO-TeA, 100 ng/L for
142 PFO2HxA, PFO3OA, PFO5DoA and HFPO-TA, and 10 ng/L for all other PFASs.

143

144 **Text S3. Quality assurance/quality control (QA/QC) for LC-MS analysis**

145 QC samples included instrument blanks (no isotopically labeled internal standard added), method
146 blanks, initial calibration verification (ICV) samples at 500 ng/L using standards from a second
147 source when possible, and continuing calibration verification (CCV) samples at 500 ng/L.
148 Accuracies of ICVs and CCVs ranged from 82-110% and 72-113%, respectively. Instrument
149 blanks (90:10 water:methanol) were run between samples to verify that the instrument was clean
150 and that there was no carry over after the highest calibration point. The storage time for samples
151 was up to three weeks at room temperature (20.2°C). Approximately 20% of samples were
152 analyzed in duplicate and concentrations of PFASs had relative standard deviations (RSD) of
153 <20% across replicates.

154

155 **Text S4. Headspace gas chromatography-mass spectrometry (GC-MS) method for** 156 **Fluoroethers E-1, E-2, and E-3**

157 Concentrations of Fluoroethers E-1, E-2, and E-3 were measured in triplicate by GC-MS using
158 headspace analysis using a method similar to previously developed methods.⁴ Triplicate
159 measurements were taken to assess variability in analyte response as mass-labeled standards were
160 not available for Fluoroether E-1, E-2, and E-3. Samples were prepared in 20-mL headspace vials
161 containing 10 mL of ultrapure water and 2.5 g sodium chloride. Ten microliters of either an
162 experimental sample or calibration standard was collected using a gas-tight syringe and injected
163 into the saline water, after which the vial was immediately capped and gently mixed. A headspace
164 autosampler (CTC Analytics CombiPal) was used to first heat the sample to 60°C for 10 minutes
165 with intermittent shaking (5 seconds at 500 rpm then 2 seconds rest). Then a syringe heated to
166 65°C was used to withdraw 300 μ L of headspace from the vial and inject it into the GC-MS
167 (Agilent 7890 GC, Agilent 7010 MS). Using helium (0.7 mL/min) as the carrier gas, analytes were
168 separated on a DB 624 Ultra Inert column (20 m x 0.18 mm x 1.00 μ m, J&W). The GC oven

169 program began at 35°C, held for 0.75 minutes, then ramped to 240°C at 15°C/min. Compounds
170 were ionized with an electron ionization (EI) MS source at 70 eV. Selected-ion monitoring (SIM)
171 was used to quantify Fluoroethers with the most prevalent ion in each spectrum ($m/z = 101, 169,$
172 and 169 for Fluoroethers E-1, E-2, and E-3 respectively). Compound retention time (1.13, 1.61,
173 and 2.61 min for Fluoroether E-1, E-2, and E-3 respectively) and the ratios of major to minor ions
174 were used to verify compound identity. Weighted 4-point calibration curves were developed in
175 duplicate for each compound, and calibration standards were prepared in the solvent considered in
176 each experiment (i.e. ACN, acetone, and DMSO) prior to dilution into saline water as described
177 above.

178 To verify that volatile losses of Fluoroethers E-1, E-2, and E-3 were negligible from headspace-
179 free containers containing the solvent of interest, 5-day experiments were conducted by adding a
180 mix of Fluoroethers E-1, E-2, and E-3 to solvent (ACN, acetone, or DMSO) in a 25 mL volumetric
181 flask. The volumetric flask was inverted twice to fully mix PFASs, and the first sample set ($t_0,$
182 $n=3$, analyzed and quantified on GC-MS) was taken immediately after mixing. A separate set of
183 5-day samples ($n=3$) was prepared and transferred to a 20-mL headspace-free amber glass vial and
184 stored for 5 days. The last sample ($t=5$ days) was taken and analyzed following the headspace GC-
185 MS method. Results indicated no statistically significant difference (t-test, $n=3$, $p>0.05$) in
186 concentrations between samples collected at t_0 and $t=5$ days.

187
188 To understand mechanisms of HFPO-DA, HFPO-TA, and HFPO-TeA degradation to Fluoroethers
189 E-1, E-2, and E-3, respectively, in polar aprotic solvents (e.g. acetone), we conducted experiments
190 with (1) HFPO-DA, (2) HFPO-TA, (3) HFPO-TeA, and (4) mix of Fluoroethers E-1, E-2, and E-
191 3 (control experiment) in fully deuterated acetone (acetone-D6). The purpose of the control
192 experiment with Fluoroethers E-1, E-2, and E-3 was to verify that the deuterium in acetone-D6 did
193 not exchange with the native hydrogen in Fluoroethers E-1, E-2, and E-3. Briefly, an aliquot of an
194 individual HFPO acid was added to acetone-D6 in a 2-mL glass vial, yielding a starting
195 concentration of ~ 2 g/L. After ~ 2 days at room temperature in the dark, ten microliters of sample
196 from the glass vial was transferred to a 20-mL headspace vial. Samples were analyzed in triplicate
197 by GC-MS using headspace analysis as described above, except that no water was included in
198 headspace vials to minimize the potential for deuterium to exchange with native hydrogen from
199 the water. Chemical ionization was used with methane (1 mL/min) as the reagent gas and 125 eV

200 ionization energy. The source was held at 300°C and the quadrupoles at 150°C. Selected-ion
201 monitoring (SIM) was used to quantify the $[M-F]^+$ for each compound (m/z of 267, 433, and 599
202 for Fluoroethers E-1, E-2, and E-3, respectively) as well as $[M-F+1]^+$ for each compound (m/z of
203 268, 434, and 600 for Fluoroethers E-1, E-2, and E-3, respectively).

204

205 **Text S5. Gas chromatography-high resolution mass spectrometry (GC-HRMS) analysis for** 206 **degradation product identification**

207 Samples diluted into 10-mL saline water in 20-mL headspace vials (see Text S4) were further
208 analyzed by GC-HRMS to identify suspected degradation products of PMPA, PEPA, PFO2HxA,
209 PFO3OA, PFO4DA, and PFO5DoA. Standards of Fluoroethers E-1, E-2, and E-3 were run along
210 with the HFPO-DA, HFPO-TA, and HFPO-TeA samples as checks that methods were suitable for
211 these products. Using a Thermo Scientific (Waltham, MA) TriPlus RSH autosampler, the same
212 headspace method from Text S4 was employed; briefly, a 2.5-mL syringe at 65°C sampled 300
213 μ L of headspace after 10-min incubation at 60°C with agitation (5 seconds on, 2 seconds off). The
214 300 μ L were injected into a Thermo Trace 1300 GC coupled to a Q Exactive GC Orbitrap MS.
215 The GC inlet was maintained at 200 °C with a split flow of 5 mL/min and helium carrier gas flow
216 rate of 1.0 mL/min (5:1 split ratio). GC separations were performed using an Agilent DB-624 (30
217 m \times 0.25 mm \times 1.40 μ m) capillary column. The 14.4-min oven program began at an initial
218 temperature of 35°C held for 0.75 min, then ramped at 15°C/min to 240 °C, with a transfer line
219 temperature of 250°C. Two ionization modes were utilized, electron ionization (EI) and chemical
220 ionization (CI), using an EI/CI combination ion source. Both methods used a source temperature
221 of 270°C and electron energy of 70 eV. The Orbitrap mass analyzer was used for full scan
222 acquisition from 60-650 m/z at 60,000 resolving power. In the CI method only, methane reagent
223 gas (1.5 mL/min) was used to conduct positive CI analyses.

224 For initial discovery of products, samples were run using EI; its high-signal total ion chromatogram
225 (TIC) facilitated visual recognition of degradation product peaks by comparison of samples to
226 solvent blanks. EI is a hard ionization technique, and the products found provided little molecular
227 information, aside from presence of common perfluoro-terminal fragments (e.g., CF_3^+ [68.9946
228 m/z]). For more structural information, positive CI was used to target more-intact, higher
229 molecular weight fragments of products that eluted at retention times as determined by EI analyses.
230 The most intact fragments tended to be $[M-F]^+$ for the compounds assessed.

231 The suspected decarboxylated-PMPA degradation product was later confirmed by retention time
232 and mass spectral matching to a standard of 1,2,2,2-tetrafluoroethyl trifluoromethyl ether (HFE
233 227), but was not quantified due to the complexity associated with making quantitative
234 measurements using gaseous standards.

235 Because no degradation products could be determined for the multi-ether PFECAs (PFO2HxA,
236 PFO3OA, PFO4DA, and PFO5DoA), higher concentration (1 µg/mL) samples were prepared in
237 acetone (10 mL in 20-mL headspace vials) from both methanol and water stocks (0.1%, pH>7)
238 and stored at room temperature. EI-GC-Orbitrap analyses were performed periodically over the
239 course of a month, with time points spanning from minutes to weeks after acetone-dilution. Despite
240 the quantified disappearance of the parent ether acids, headspace GC-MS analyses did not reveal
241 any apparent volatile degradation products formed, even in these higher-concentration samples.
242 To assess the potential formation of nonvolatile or thermally labile degradation products for these
243 compounds, a liquid-injection GC-MS method was also used on these same high-concentration
244 samples. In this method, 1 µL of multi-ether PFECA sample in acetone was injected into a
245 programmable temperature vaporizing (PTV) inlet at 60°C, which was then ramped at 14.5°C/s to
246 150°C for a 1 min transfer step followed by a 2 min cleaning step at 250°C. Still, no byproducts
247 were identified using this method. It is possible that products might elute with the solvent, making
248 them nearly impossible to find, especially when performing unknown analysis. Compared to other
249 PFEAs in this study (e.g., HFPO-DA) that favored one major degradation product, it is also
250 possible that solvent-facilitated degradation of the multi-ether PFECAs resulted in a variety of
251 products, which would have lower abundance in GC-MS analyses, perhaps below limit of
252 detection (LOD).

253

254 **Text S6. First-order kinetics**

255 The degradation of branched mono-ether PFECAs and multi-ether PFECAs in ACN, acetone, and
256 DMSO can be expressed by first-order kinetics [Equations (1) and (2)], where k is the observed
257 first-order rate constant, t is time, $[PFAS]$ is PFAS concentration, and $[PFAS]_0$ is the initial PFAS
258 concentration.

$$259 \quad \frac{d[PFAS]}{dt} = -k[PFAS] \quad (1)$$

260 Integration yields:

261
$$\ln \left(\frac{[\text{PFAS}]}{[\text{PFAS}]_0} \right) = -kt \quad (2)$$

262 The k values were obtained from slopes of linear regression lines describing experimental $\ln(C/C_0)$
263 values as a function of time.

264

265 **Text S7. Arrhenius equation**

266 The temperature-dependence of first-order rate constants describing the degradation of branched
267 mono-ether PFECAs in ACN, acetone, and DMSO was described by the Arrhenius equation:

268
$$k = Ae^{-E_a/RT} \quad (3)$$

269 which was linearized to give:

270
$$\ln k = \ln A - \frac{E_a}{RT} \quad (4)$$

271 where k is the temperature-dependent first-order rate constant, A is the pre-exponential factor, E_a
272 is the activation energy, R is the universal gas constant ($8.314 \text{ J K}^{-1} \text{ mol}^{-1}$), and T is absolute
273 temperature in Kelvin.

274

275 **Text S8. Calculation of molar yield**

276 Molar yield of Fluoroethers E-1, E-2, and E-3 from HFPO-DA, HFPO-TA, and HFPO-TeA,
277 respectively, in acetonitrile (ACN), acetone, and dimethyl sulfoxide (DMSO) after 5 days is shown
278 in Table S12 and calculated from the following equation:

279
$$[\text{Product}]/[\text{PFECA}]_0 = \frac{\bar{b}}{\bar{a}} \pm \frac{\bar{b}}{\bar{a}} \sqrt{\left(\frac{S_a}{\bar{a}}\right)^2 + \left(\frac{S_b}{\bar{b}}\right)^2}$$

280 where \bar{a} and \bar{b} are the average concentrations of PFECAs (i.e. HFPO-DA, HFPO-TA, or HFPO-
281 TeA) and Fluoroethers (i.e. E-1, E-2, or E-3) in replicate measurements, respectively; S_a and S_b
282 are standard deviations of concentrations of PFECAs (i.e. HFPO-DA, HFPO-TA, or HFPO-TeA)
283 and Fluoroethers (i.e. E-1, E-2, or E-3) in replicate measurements, respectively.

284

285

286 **Table S1. Per- and polyfluoroalkyl substances (PFASs) targeted in this study**

Analyte	Formula	CAS # (hyperlinked to US EPA Chemicals Dashboard)	Source ^a	Mass-Labeled Internal Standard	Solvent
Class 1: Perfluorocarboxylic acids (PFCA)					
Perfluorohexanoic acid (PFHxA)	C ₆ HF ₁₁ O ₂	307-24-4	1	¹³ C ₅ -PFHxA	Methanol
Class 2: Perfluorosulfonic acids (PFSA)					
Perfluorohexane sulfonic acid (PFHxS)	C ₆ HF ₁₃ SO ₃	355-46-4	1	¹³ C ₃ -PFHxS	Methanol
Class 3: Per- and polyfluoroalkyl ether acids (PFEAs)					
Perfluoroalkyl mono-ether carboxylic acids (mono-ether PFECAs)					
Perfluoro-2-methoxyacetic acid (PFMOAA)	C ₃ HF ₅ O ₃	674-13-5	2, 3	¹³ C ₄ -PFBA	Basic methanol ^b
Perfluoro-3-methoxypropanoic acid (PFMOPrA) ^c	C ₄ HF ₇ O ₃	377-73-1	4	¹³ C ₄ -PFBA	Methanol
Perfluoro-2-methoxypropanoic acid (PMPA)	C ₄ HF ₇ O ₃	13140-29-9	3	¹³ C ₄ -PFBA	Deionized water
Perfluoro-4-methoxybutanoic acid (PFMOBA) ^c	C ₅ HF ₉ O ₃	863090-89-5	4	¹³ C ₅ -PFHxA	Methanol
Perfluoro-2-ethoxypropanoic acid (PEPA)	C ₅ HF ₉ O ₃	267239-61-2	3	¹³ C ₅ -PFHxA	Deionized water
Hexafluoropropylene oxide-dimer acid (HFPO-DA) = Perfluoro-2-propoxypropanoic acid (PFPrOPrA)	C ₆ HF ₁₁ O ₃	13252-13-6	4, 5	¹³ C ₃ -PFPrOPrA	Methanol
Ammonium salt of hexafluoropropylene oxide-dimer acid = "GenX"	C ₆ H ₄ F ₁₁ NO ₃	62037-80-3	4	¹³ C ₃ -PFPrOPrA	Methanol
Perfluoroalkyl multi-ether carboxylic acids (multi-ether PFECAs)					
Perfluoro(3,5-dioxahexanoic) acid (PFO2HxA)	C ₄ HF ₇ O ₄	39492-88-1	3	¹³ C ₃ -PFPrOPrA	Deionized water
Perfluoro(3,5,7-trioxaoctanoic) acid (PFO3OA)	C ₅ HF ₉ O ₅	39492-89-2	3	¹³ C ₃ -PFPrOPrA	Deionized water
Perfluoro(3,5,7,9-tetraoxadecanoic) acid (PFO4DA)	C ₆ HF ₁₁ O ₆	39492-90-5	3	¹³ C ₃ -PFPrOPrA	Deionized water

Perfluoro(3,5,7,9,11-pentaoxadodecanoic) acid (PFO5DoA)	C ₇ HF ₁₃ O ₇	39492-91-6	3	¹³ C ₃ -PFPrOPrA	Deionized water
Hexafluoropropylene oxide-trimer acid (HFPO-TA)	C ₉ HF ₁₇ O ₄	13252-14-7	4	¹³ C ₃ -PFPrOPrA	Methanol
Hexafluoropropylene oxide-tetramer acid (HFPO-TeA)	C ₁₂ HF ₂₃ O ₅	65294-16-8	4	¹³ C ₃ -PFPrOPrA	Methanol

Polyfluoroalkyl ether acids

Ethanesulfonic acid, 2-[1-[difluoro(1,2,2,2-tetrafluoroethoxy)methyl]-1,2,2,2-tetrafluoroethoxy]-1,1,2,2-tetrafluoro- (Nafion by-product 2)	C ₇ H ₂ F ₁₄ SO ₅	749836-20-2	3, 4	¹³ C ₃ -PFHxS	Methanol
1,1,2,2-tetrafluoro-2-(1,2,2,2-tetrafluoro-ethoxy)ethane sulfonate (NVHOS)	C ₄ H ₂ F ₈ SO ₄	801209-99-4	3	¹³ C ₃ -PFBS	Deionized water
2,2,3,3-tetrafluoro-3-((1,1,1,2,3,3-hexafluoro-3-(1,2,2,2-tetrafluoroethoxy)propan-2-yl)oxy)propanoic acid (HydroEVE)	C ₈ H ₂ F ₁₄ O ₄	773804-62-9	3	¹³ C ₃ -PFPrOPrA	Deionized water
4,8-dioxa-3H-perfluorononanoic acid (ADONA)	C ₇ H ₂ F ₁₂ O ₄	919005-14-4	1	¹³ C ₄ -PFOA	Methanol
9-chlorohexadecafluoro-3-oxanone-1-sulfonic acid (9Cl-PF3ONS, main component of F-53B)	C ₈ HF ₁₆ SO ₄ Cl	756426-58-1	1	¹³ C ₄ -PFOS	Methanol

Class 4: Fluorotelomer sulfonate

6:2 fluorotelomer sulfonate (6:2 FtS)	C ₈ H ₅ F ₁₃ O ₃ S	27619-97-2	1, 4	¹³ C ₂ -6:2 FtS	Methanol
---------------------------------------	--	----------------------------	------	---------------------------------------	----------

287 ^a Source: 1 Wellington Laboratories (Guelph, ON, Canada), 2 Fluorox Labs (Carson City, NV), 3 The Chemours Company (Wilmington, DE), 4 SynQuest

288 Laboratories (Alachua, FL), 5 Cambridge Isotope Laboratories (Tewksbury, MA).

289 ^b Basic methanol: 95% methanol + 5% deionized water with 2.5 M NaOH

290 ^c Highlighted chemicals indicate structural isomers. See Figure S1.

291

292 **Table S2. Structures of 1,2,2,2-Tetrafluoroethyl trifluoromethyl ether and Fluoroethers E-1,**
 293 **E-2, and E-3**

Compound	Formula	CAS #	Molecular structure
1,2,2,2-Tetrafluoroethyl trifluoromethyl ether (HFE 227)*	C ₃ HF ₇ O	2356-62-9	
Heptafluoropropyl 1,2,2,2-tetrafluoroethyl ether (Fluoroether E-1)*	C ₅ HF ₁₁ O	3330-15-2	
2H-Perfluoro-5-methyl-3,6-dioxanonane (Fluoroether E-2)*	C ₈ HF ₁₇ O ₂	3330-14-1	
2H-Perfluoro-5,8-dimethyl-3,6,9-trioxadodecane (Fluoroether E-3)*	C ₁₁ HF ₂₃ O ₃	3330-16-3	

294 * Source: SynQuest Laboratories (Alachua, FL).

295

296 **Table S3. Stability of PFASs in deionized water at room temperature (20.2°C) for 7 and 30**
 297 **days**

Compound	Initial concentration (µg/L)	Day 7 mean % recovery ^a	Day 7 % RSD ^b	Day 30 mean % recovery	Day 30 % RSD
PFHxA	50.6	98.3	1.6	93.0	3.9
PFHxS	49.8	95.3	1.8	90.7	5.4
PFMOAA	57.2	99.3	0.4	94.1	0.7
PFMOPrA	39.3	95.5	1.2	90.4	0.1
PMPA	46.6	94.0	1.5	95.3	7.2
PFMOBA	49.1	97.3	1.1	94.7	8.7
PEPA	46.9	92.3	2.9	96.2	5.6
HFPO-DA (PFPrOPrA)	44.2	94.6	4.0	94.8	11.1
GenX	26.5	95.0	0.2	91.0	10.5
PFO2HxA	43.1	97.4	2.3	97.8	0.2
PFO3OA	42.3	92.6	1.8	92.6	3.9
PFO4DA	41.3	95.8	0.1	89.8	2.0
PFO5DoA	41.0	99.2	4.6	95.0	3.5
HFPO-TA	38.0	99.2	9.9	94.7	1.2
HFPO-TeA	29.3	95.6	1.2	109.7	8.2
Nafion by-product 2	38.6	96.1	0.1	91.7	4.0
NVHOS	56.3	94.9	0.5	96.3	12.6
HydroEVE	34.5	101.1	2.7	102.5	3.7
ADONA	28.4	99.6	2.3	93.5	1.9
F-53B	50.1	102.3	1.9	104.0	14.8
6:2 FtS	40.8	99.5	3.9	102.2	0.8

298 ^a For ease of data comparison, all analyte concentrations were normalized to the initial concentration and converted to
 299 percent recoveries.

300 ^b Relative standard deviation (RSD) represents for duplicate measurements.

301

302 **Table S4. Stability of PFASs in methanol at room temperature (20.2°C) for 7 and 30 days**

Compound	Initial concentration (µg/L)	Day 7 mean % recovery ^a	Day 7 % RSD ^b	Day 30 mean % recovery	Day 30 % RSD
PFHxA	50.5	92.1	3.1	97.8	8.0
PFHxS	49.1	97.5	0.5	100.4	1.9
PFMOAA	51.4	104.6	1.5	96.7	1.5
PFMOPrA	43.0	105.4	3.2	97.0	1.4
PMPA	48.0	92.4	3.4	99.5	6.7
PFMOBA	48.0	106.1	5.2	97.0	0.4
PEPA	49.7	92.2	4.1	95.0	2.8
HFPO-DA (PFPrOPrA)	40.9	94.5	5.8	101.5	4.1
GenX	26.8	100.7	4.4	92.3	2.3
PFO2HxA	46.0	95.4	4.8	105.2	7.0
PFO3OA	43.5	93.0	4.9	96.4	2.5
PFO4DA	45.9	92.0	5.8	94.5	4.4
PFO5DoA	46.9	92.9	2.1	98.6	4.9
HFPO-TA	30.7	103.5	1.3	103.2	8.4
HFPO-TeA	34.6	91.8	13.9	93.2	2.9
Nafion by-product 2	44.6	98.9	5.6	101.8	0.9
NVHOS	45.3	96.5	1.6	102.7	2.8
HydroEVE	45.9	93.7	6.1	97.9	5.9
ADONA	28.3	106.5	3.4	103.0	6.7
F-53B	39.0	113.4	7.8	96.1	14.3
6:2 FtS	43.8	101.1	4.8	102.1	5.3

303 ^a For ease of data comparison, all analyte concentrations were normalized to the initial concentration and converted to
 304 percent recoveries.

305 ^b Relative standard deviation (RSD) represents for duplicate measurements.

306

307

308 **Table S5. Stability of PFASs in isopropyl alcohol (IPA) at room temperature (20.2°C) for 7**
 309 **and 30 days**

Compound	Initial concentration (µg/L)	Day 7 mean % recovery ^a	Day 7 % RSD ^b	Day 30 mean % recovery	Day 30 % RSD
PFHxA	50.0	95.9	13.7	99.4	12.4
PFHxS	57.6	95.2	6.8	98.6	4.2
PFMOAA	47.2	106.9	3.8	101.1	3.7
PFMOPrA	40.6	112.2	8.6	107.0	9.5
PMPA	49.8	89.5	12.5	95.3	1.5
PFMOBA	42.5	110.1	9.6	104.3	12.5
PEPA	50.7	90.9	12.6	94.5	1.2
HFPO-DA (PFPrOPrA)	48.8	91.6	10.0	98.9	4.3
GenX	24.3	111.8	9.8	109.9	15.9
PFO2HxA	47.6	96.0	11.6	98.1	2.8
PFO3OA	43.4	107.3	5.7	110.4	0.8
PFO4DA	44.2	100.1	6.1	104.7	3.5
PFO5DoA	48.3	101.5	2.6	96.0	3.3
HFPO-TA	35.8	107.6	10.5	110.6	9.2
HFPO-TeA	31.5	90.2	5.4	99.4	3.1
Nafion by-product 2	50.1	102.3	6.0	102.7	5.8
NVHOS	45.0	95.1	9.3	101.9	2.7
HydroEVE	48.3	99.6	5.5	103.3	2.9
ADONA	25.0	119.2	14.8	108.1	7.6
F-53B	54.1	120.1	7.5	108.0	3.5
6:2 FtS	42.6	97.1	3.0	105.0	4.5

310 ^a For ease of data comparison, all analyte concentrations were normalized to the initial concentration and converted to
 311 percent recoveries.

312 ^b Relative standard deviation (RSD) represents for duplicate measurements.

313

314 **Table S6. Stability of PFASs in acetonitrile (ACN) at room temperature (20.2°C) for 7 and**
 315 **30 days**

Compound	Initial concentration (µg/L)	Day 7 mean % recovery ^a	Day 7 % RSD ^b	Day 30 mean % recovery ^b	Day 30 % RSD ^c
PFHxA	54.8	95.5	2.1	92.8	10.2
PFHxS	50.0	96.3	2.0	96.4	4.3
PFMOAA	34.7	105.7	2.1	97.6	11.7
PFMOPrA	31.2	107.4	1.2	110.3	7.7
PMPA	52.1	ND ^c	ND	ND	ND
PFMOBA	47.5	104.0	2.0	101.9	2.3
PEPA	54.9	ND	ND	ND	ND
HFPO-DA (PFPrOPrA)	36.6	ND	ND	ND	ND
GenX	48.5	ND	ND	ND	ND
PFO2HxA	50.5	87.5	3.4	66.8	1.7
PFO3OA	34.6	89.3	5.2	65.8	2.5
PFO4DA	57.2	86.5	0.6	59.6	2.0
PFO5DoA	54.0	92.8	10.8	67.5	4.2
HFPO-TA	30.8	ND	ND	ND	ND
HFPO-TeA	20.1	ND	ND	ND	ND
Nafion by-product 2	46.4	101.3	4.1	99.6	6.4
NVHOS	47.6	95.4	2.2	96.2	3.8
HydroEVE	48.4	93.0	3.3	97.8	10.0
ADONA	27.3	104.7	6.7	100.2	5.6
F-53B	43.4	103.2	3.3	106.1	8.2
6:2 FtS	51.0	97.0	0.7	102.0	10.1

316 ^a For ease of data comparison, all analyte concentrations were normalized to the initial concentration and converted to
 317 percent recoveries.

318 ^b Relative standard deviation (RSD) represents for duplicate measurements.

319 ^c ND means concentration is below quantitation limit (QL).

320

321 **Table S7. Stability of PFASs in acetone at room temperature (20.2°C) for 7 and 30 days**

Compound	Initial concentration (µg/L)	Day 7 mean % recovery ^a	Day 7 % RSD ^b	Day 30 mean % recovery	Day 30 % RSD
PFHxA	44.4	95.1	6.4	99.6	10.6
PFHxS	50.4	97.5	2.8	93.1	6.0
PFMOAA	55.4	109.9	0.8	96.8	3.2
PFMOPrA	46.2	103.8	1.1	110.9	8.3
PMPA	49.5	ND ^c	ND	ND	ND
PFMOBA	57.4	109.7	2.2	110.2	17.2
PEPA	51.6	ND	ND	ND	ND
HFPO-DA (PFPrOPrA)	44.7	ND	ND	ND	ND
GenX	50.3	ND	ND	ND	ND
PFO2HxA	38.4	66.4	1.5	18.7	1.1
PFO3OA	42.4	54.0	1.5	10.9	2.1
PFO4DA	48.3	41.3	1.2	ND	ND
PFO5DoA	43.7	60.5	0.4	ND	ND
HFPO-TA	31.0	ND	ND	ND	ND
HFPO-TeA	29.2	ND	ND	ND	ND
Nafion by-product 2	41.3	101.4	3.0	95.3	3.3
NVHOS	41.9	100.9	4.1	95.6	6.5
HydroEVE	41.7	96.6	4.6	100.1	8.9
ADONA	29.4	103.5	0.6	100.5	7.3
F-53B	55.7	97.4	12.6	104.8	14.7
6:2 FtS	44.3	101.8	9.8	109.0	9.5

322 ^a For ease of data comparison, all analyte concentrations were normalized to the initial concentration and converted to
 323 percent recoveries.

324 ^b Relative standard deviation (RSD) represents for duplicate measurements.

325 ^c ND means concentration is below quantitation limit (QL).

326

327 **Table S8. Stability of PFASs in dimethyl sulfoxide (DMSO) at room temperature (20.2°C)**
 328 **for 7 and 30 days**

Compound	Initial concentration (µg/L)	Day 7 mean % recovery ^a	Day 7 % RSD ^b	Day 30 mean % recovery	Day 30 % RSD
PFHxA	55.8	97.2	1.6	94.4	10.5
PFHxS	58.6	96.4	3.4	95.3	1.5
PFMOAA	68.8	105.3	2.1	95.1	6.1
PFMOPrA	46.6	109.7	3.0	92.1	4.8
PMPA	41.3	ND ^c	ND	ND	ND
PFMOBA	57.8	100.4	2.4	96.1	3.0
PEPA	40.5	ND	ND	ND	ND
HFPO-DA (PFPrOPrA)	45.7	ND	ND	ND	ND
GenX	57.1	ND	ND	ND	ND
PFO2HxA	42.4	89.3	1.3	58.4	1.3
PFO3OA	43.2	83.2	0.6	51.9	0.4
PFO4DA	43.4	86.3	1.4	60.0	8.9
PFO5DoA	46.6	89.9	4.1	62.8	1.4
HFPO-TA	34.8	ND	ND	ND	ND
HFPO-TeA	25.4	ND	ND	ND	ND
Nafion by-product 2	50.5	90.8	4.7	95.4	3.8
NVHOS	57.8	93.2	4.1	93.3	2.0
HydroEVE	53.3	92.9	7.7	103.4	4.7
ADONA	27.6	109.2	2.6	103.8	1.6
F-53B	48.4	99.9	19.6	100.1	2.0
6:2 FtS	46.2	106.4	6.7	108.0	0.2

329 ^a For ease of data comparison, all analyte concentrations were normalized to the initial concentration and converted to
 330 percent recoveries.

331 ^b Relative standard deviation (RSD) represents for duplicate measurements.

332 ^c ND means concentration is below quantitation limit (QL).

333

334 **Table S9. Summary of the stability of PFASs targeted in this study**

Class	Compound	Solvent			
		Acetonitrile (ACN)	Acetone	Dimethyl sulfoxide (DMSO)	Polar protic solvents ^a
PFCA	PFHxA	No deg. ^b	No deg.	No deg.	No deg.
PFSA	PFHxS	No deg.	No deg.	No deg.	No deg.
Mono-ether PFECAs	PFMOAA	No deg.	No deg.	No deg.	No deg.
	PFMOPrA	No deg.	No deg.	No deg.	No deg.
	PMPA	$k = 3.03 \text{ d}^{-1}$ ^c	$k = 19.2 \text{ d}^{-1}$	$k = 2.00 \text{ d}^{-1}$	No deg.
	PFMOBA	No deg.	No deg.	No deg.	No deg.
	PEPA	$k = 4.75 \text{ d}^{-1}$	$k = 27.0 \text{ d}^{-1}$	$k = 2.63 \text{ d}^{-1}$	No deg.
	HFPO-DA (PFPrOPrA)	$k = 4.96 \text{ d}^{-1}$	$k = 45.4 \text{ d}^{-1}$	$k = 3.92 \text{ d}^{-1}$	No deg.
Multi-ether PFECAs	GenX	$k = 5.86 \text{ d}^{-1}$	$k = 47.9 \text{ d}^{-1}$	$k = 4.64 \text{ d}^{-1}$	No deg.
	PFO2HxA	$k = 0.0136 \text{ d}^{-1}$	$k = 0.0578 \text{ d}^{-1}$	$k = 0.0168 \text{ d}^{-1}$	No deg.
	PFO3OA	$k = 0.0128 \text{ d}^{-1}$	$k = 0.0743 \text{ d}^{-1}$	$k = 0.0195 \text{ d}^{-1}$	No deg.
	PFO4DA	$k = 0.0170 \text{ d}^{-1}$	$k = 0.106 \text{ d}^{-1}$	$k = 0.0160 \text{ d}^{-1}$	No deg.
	PFO5DoA	$k = 0.0129 \text{ d}^{-1}$	$k = 0.0732 \text{ d}^{-1}$	$k = 0.0139 \text{ d}^{-1}$	No deg.
	HFPO-TA	$k = 3.39 \text{ d}^{-1}$	$k = 27.8 \text{ d}^{-1}$	$k = 3.52 \text{ d}^{-1}$	No deg.
	HFPO-TeA	$k = 3.71 \text{ d}^{-1}$	$k = 32.1 \text{ d}^{-1}$	$k = 3.68 \text{ d}^{-1}$	No deg.
Polyfluoroalkyl ether acids	Nafion by-product 2	No deg.	No deg.	No deg.	No deg.
	NVHOS	No deg.	No deg.	No deg.	No deg.
	HydroEVE	No deg.	No deg.	No deg.	No deg.
	ADONA	No deg.	No deg.	No deg.	No deg.
	F-53B	No deg.	No deg.	No deg.	No deg.
Fluorotelomer sulfonate	6:2FtS	No deg.	No deg.	No deg.	No deg.

335 ^a All studied PFASs had no measurable degradation in the polar protic solvents water, methanol, and isopropyl alcohol
336 (IPA) in ~30 days.

337 ^b No deg. means the studied PFAS had no measurable degradation in ~30 days.

338 ^c Averages of observed first-order rate constants (k) are summarized here. See Table 2 for 95% confidence intervals.

339

340 **Table S10. First-order rate constants (*k*) of PMPA, PEPA, and HFPO-DA in acetonitrile**
 341 **(ACN), acetone, and dimethyl sulfoxide (DMSO) with different water-to-organic solvent**
 342 **ratios (100% organic solvent, 90:10% (v/v) and 80:20% (v/v) organic solvent:water) at room**
 343 **temperature (20.2°C)**

Compound	100% ACN		90% ACN+10% water		80% ACN+20% water	
	<i>k</i> (d ⁻¹)	R ²	<i>k</i> (d ⁻¹)	R ²	<i>k</i> (d ⁻¹)	R ²
PMPA	3.03 ^{a,b} (2.74, 3.31)	0.906	0.0185 (0.0172, 0.0198)	0.988	No measurable degradation in 30 d	
PEPA	4.75 ^b (4.41, 5.10)	0.945	0.0267 (0.0240, 0.0295)	0.974	No measurable degradation in 30 d	
HFPO-DA (PFPrOPrA)	4.96 ^b (4.39, 5.52)	0.882	0.0380 (0.0342, 0.0417)	0.978	No measurable degradation in 30 d	
Compound	100% Acetone		90% Acetone +10% water		80% Acetone +20% water	
	<i>k</i> (d ⁻¹)	R ²	<i>k</i> (d ⁻¹)	R ²	<i>k</i> (d ⁻¹)	R ²
PMPA	19.2 ^b (17.1, 21.2)	0.909	0.0753 (0.0700, 0.0806)	0.989	0.0151 (0.0136, 0.0166)	0.977
PEPA	27.0 ^b (24.7, 29.3)	0.943	0.128 (0.123, 0.0133)	0.997	0.0260 (0.0242, 0.0278)	0.988
HFPO-DA (PFPrOPrA)	45.4 ^b (43.5, 47.3)	0.988	0.192 (0.155, 0.228)	0.965	0.0329 (0.0296, 0.0362)	0.975
Compound	100% DMSO		90% DMSO +10% water		80% DMSO +20% water	
	<i>k</i> (d ⁻¹)	R ²	<i>k</i> (d ⁻¹)	R ²	<i>k</i> (d ⁻¹)	R ²
PMPA	2.00 ^b (1.73, 2.27)	0.826	0.299 (0.262, 0.335)	0.985	0.0471 (0.0425, 0.0518)	0.976
PEPA	2.63 ^b (2.28, 2.97)	0.838	0.473 (0.412, 0.535)	0.983	0.0587 (0.0562, 0.0611)	0.996
HFPO-DA (PFPrOPrA)	3.92 ^b (3.34, 4.51)	0.819	0.481 (0.313 0.649)	0.987	0.109 (0.101, 0.117)	0.996

344 ^a Experimental results were analyzed using the regression data analysis tool in Microsoft Excel, and the average rate
 345 constant was reported. Values in parentheses represent the lower and upper limit of 95% confidence interval.

346 ^b Experiments were conducted in replicate starting at different initial concentrations (10, 50 and 100 µg/L).

347

348 **Table S11. First-order rate constants (*k*) of PMPA, PEPA, and HFPO-DA in acetonitrile**
 349 **(ACN), acetone, and dimethyl sulfoxide (DMSO) at three temperatures [cold (3.4°C), room**
 350 **(20.2°C), and hot (32.4°C)]**

Compound	ACN, cold		ACN, room		ACN, hot	
	<i>k</i> (d ⁻¹)	R ²	<i>k</i> (d ⁻¹)	R ²	<i>k</i> (d ⁻¹)	R ²
PMPA	0.278 ^a (0.242, 0.313)	0.960	3.03 ^b (2.74, 3.31)	0.906	26.0 (24.3, 27.8)	0.996
PEPA	0.336 (0.309, 0.365)	0.983	4.75 ^b (4.41, 5.10)	0.945	29.8 (27.0, 32.6)	0.991
HFPO-DA (PFPrOPrA)	0.383 (0.365, 0.401)	0.994	4.96 ^b (4.39, 5.52)	0.882	31.8 (27.1, 36.6)	0.978
Compound	Acetone, cold		Acetone, room		Acetone, hot	
	<i>k</i> (d ⁻¹)	R ²	<i>k</i> (d ⁻¹)	R ²	<i>k</i> (d ⁻¹)	R ²
PMPA	1.11 (1.00, 1.23)	0.976	19.2 ^b (17.1, 21.2)	0.909	127 (117,138)	0.999
PEPA	1.88 (1.68, 2.07)	0.976	27.0 ^b (24.7, 29.3)	0.943	160 ^c (103, 213)	0.999
HFPO-DA (PFPrOPrA)	1.97 (1.70, 2.23)	0.960	45.4 ^b (43.5, 47.3)	0.988	191 ^c (116, 266)	0.997
Compound	DMSO, cold ^d		DMSO, room		DMSO, hot	
	<i>k</i> (d ⁻¹)	R ²	<i>k</i> (d ⁻¹)	R ²	<i>k</i> (d ⁻¹)	R ²
PMPA	-	-	2.00 ^b (1.73, 2.27)	0.826	20.0 (17.9, 22.0)	0.992
PEPA	-	-	2.63 ^b (2.28, 2.97)	0.838	24.9 (22.7, 27.0)	0.994
HFPO-DA (PFPrOPrA)	-	-	3.92 ^b (3.34, 4.51)	0.819	43.6 (29.1, 58.1)	0.968

351 ^a Experimental results were analyzed using the regression data analysis tool in Microsoft Excel, and the average rate
 352 constant was reported. Values in parentheses represent the lower and upper limit of 95% confidence interval.

353 ^b Experiments were conducted in replicate starting at different initial concentrations (10, 50 and 100 µg/L).

354 ^c The 95% confidence interval was relatively large due to the limited number of sample size (n=3; t=0, 10, and 20
 355 min).

356 ^d Experiment was not conducted at 3.4°C in DMSO due to the high melting point of DMSO (19°C).

357

358 **Table S12. Activation energy (E_a) and pre-exponential factor (A) of PMPA, PEPA, and**
 359 **HFPO-DA in acetonitrile (ACN), acetone, and dimethyl sulfoxide (DMSO)**

Compound	ACN		Acetone		DMSO ^a	
	E_a (kJ/mol)	lnA (A in d ⁻¹)	E_a (kJ/mol)	lnA (A in d ⁻¹)	E_a (kJ/mol)	lnA (A in d ⁻¹)
PMPA	108.8	46.0	114.7	50.0	140.5	58.3
PEPA	108.5	46.1	107.6	47.4	137.2	57.2
HFPO-DA (PFPrOPrA)	106.7	45.4	112.0	49.5	147.1	61.7

360 ^a Experiment was not conducted at 3.4°C in DMSO due to the high melting point of DMSO (19°C).

361
 362
 363
 364
 365 **Table S13. Molar yield of Fluoroethers E-1, E-2, and E-3 from the degradation of HFPO-**
 366 **DA, HFPO-TA, and HFPO-TeA, respectively, in acetonitrile (ACN), acetone, and dimethyl**
 367 **sulfoxide (DMSO) at room temperature (20.2°C) in 5 days**

PFAS	[PFAS] ₀	Product	[Product]	[Product]/[PFAS] ₀ ^a
Solvent: acetonitrile (ACN)				
HFPO-DA	15.6 nmol/L	Fluoroether E-1	20.1 nmol/L	129% ± 14%
HFPO-TA	9.1 nmol/L	Fluoroether E-2	8.2 nmol/L	90% ± 13%
HFPO-TeA	7.1 nmol/L	Fluoroether E-3	6.5 nmol/L	91% ± 10%
Solvent: acetone				
HFPO-DA	15.7 nmol/L	Fluoroether E-1	18.8 nmol/L	120% ± 26%
HFPO-TA	7.6 nmol/L	Fluoroether E-2	8.3 nmol/L	109% ± 16%
HFPO-TeA	7.3 nmol/L	Fluoroether E-3	7.2 nmol/L	98% ± 6%
Solvent: dimethyl sulfoxide (DMSO)				
HFPO-DA	16.4 nmol/L	Fluoroether E-1	15.1 nmol/L	92% ± 3%
HFPO-TA	11.6 nmol/L	Fluoroether E-2	9.8 nmol/L	84% ± 16%
HFPO-TeA	8.9 nmol/L	Fluoroether E-3	7.5 nmol/L	84% ± 18%

368 ^a Calculation of molar yield is detailed in Text S8.

369

370 **Table S14. The percent abundance of [M-F+1]⁺ ion for Fluoroethers E-1, E-2, and E-3 from**
 371 **the degradation of HFPO-DA, HFPO-TA, and HFPO-TeA, respectively, in fully deuterated**
 372 **acetone**

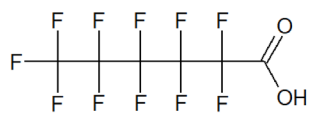
The abundance of [M-F+1] ⁺ ion to the sum abundance of [M-F] ⁺ and [M-F+1] ⁺ ions ^a	
Fluoroether E-1 (C ₅ HOF ₁₁) in deuterated acetone	Degradation product of HFPO-DA in deuterated acetone
4.8 ± 0.02%	70.2 ± 10.6%
Fluoroether E-2 (C ₈ HO ₂ F ₁₇) in deuterated acetone	Degradation product of HFPO-TA in deuterated acetone
7.7 ± 0.02%	76.4 ± 6.3%
Fluoroether E-3 (C ₁₁ HO ₃ F ₂₃) in deuterated acetone	Degradation product of HFPO-TeA in deuterated acetone
10.2 ± 0.03%	79.4 ± 5.1%

373 ^a *m/z* of [M-F]⁺ = 267 for HFPO-DA, 433 for HFPO-TA, and 599 for HFPO-TeA.

374 *m/z* of [M-F+1]⁺ = 268 for HFPO-DA, 434 for HFPO-TA, and 600 for HFPO-TeA.

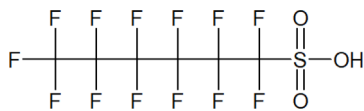
375

376



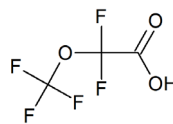
377

PFHxA

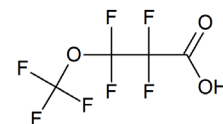


378

PFHxS

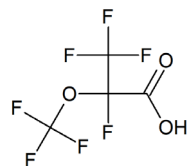


PFMOAA



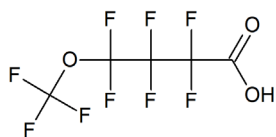
PFMOPrA

379



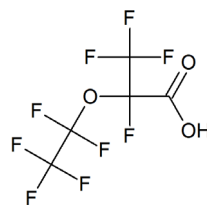
380

PMPA^a

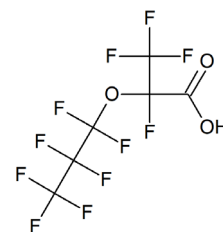


381

PFMOBA

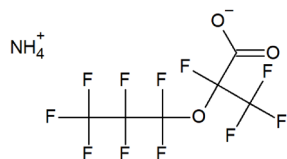


PEPA^b



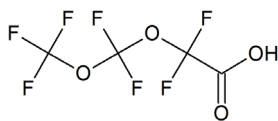
HFPO-DA (PFPrOPrA)

382



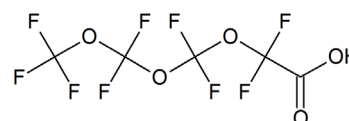
383

Ammonium salt of HFPO-DA



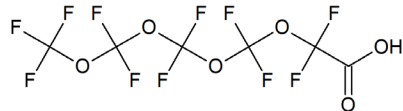
384

PFO2HxA



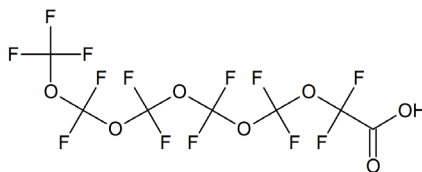
385

PFO3OA



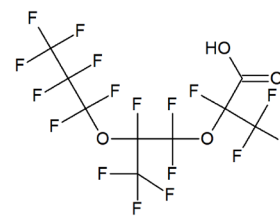
386

PFO4DA



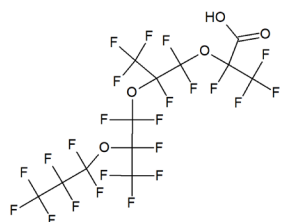
387

PFO5DoA



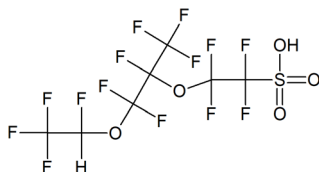
388

HFPO-TA



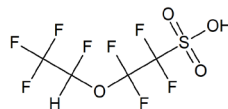
389

HFPO-TeA



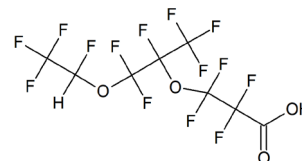
390

Nafion by-product 2



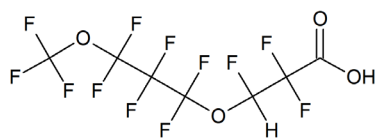
391

NVHOS

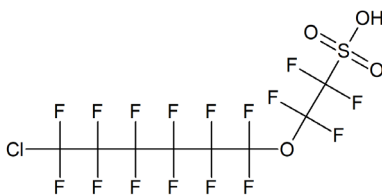


392

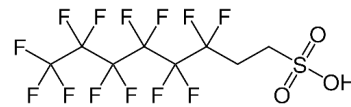
HydroEVE



ADONA



9Cl-PF3ONS (main component F-53B)



6:2 FtS

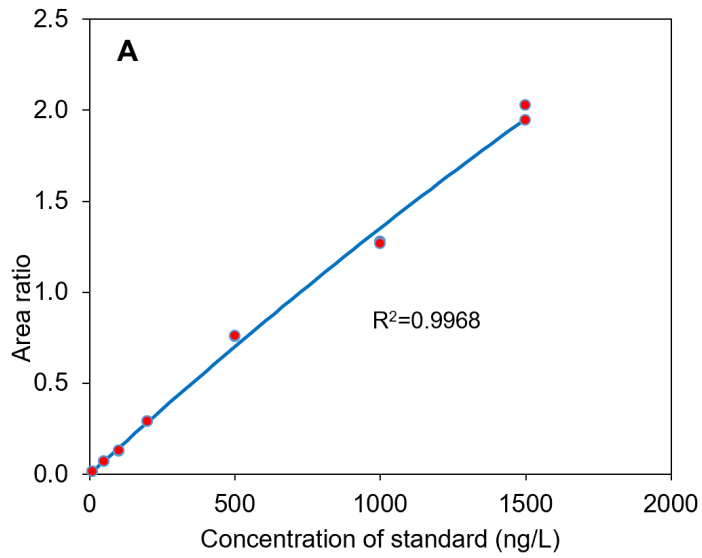
393
394
395

396 **Figure S1. Molecular structures of per- and polyfluoroalkyl substances (PFASs) evaluated**
397 **in this study.**

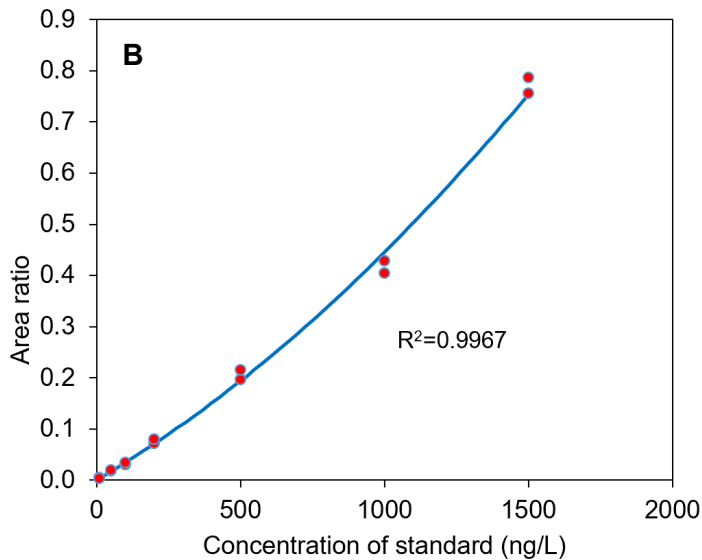
398 ^a In Sun et al. (2016),⁵ this compound was presented as PFMOPrA. However, it is likely that environmental samples
399 contain the branched isomer, PMPA, shown here and in Strynar et al. (2015).⁶

400 ^b In Sun et al. (2016),⁵ this compound was presented as PFMOBA. However, it is likely that environmental samples
401 contain the branched isomer, PEPA, shown here and in Strynar et al. (2015).⁶

402



403

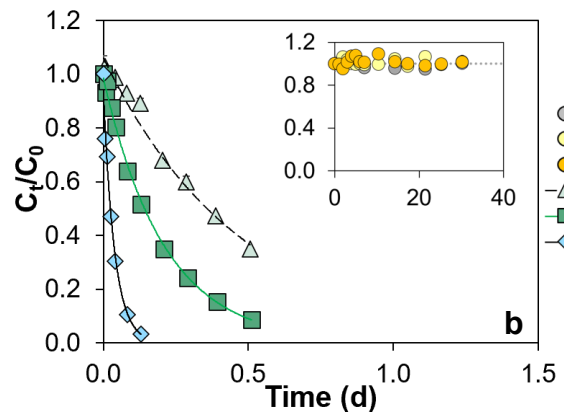
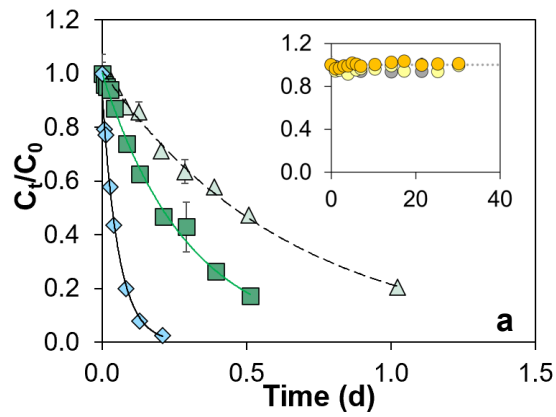


404

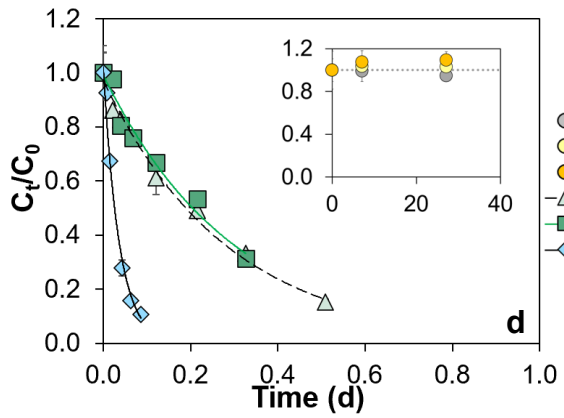
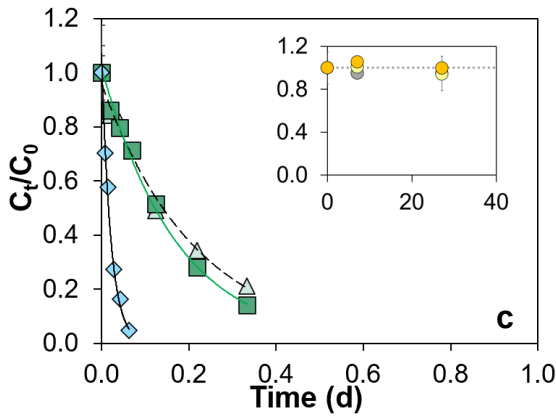
405 **Figure S2. Representative calibration curves for (A) PFHxA and (B) PFO2HxA using LC-**
406 **HRMS.**

407 Red dots represent area ratios (i.e. measured peak area for the native standard divided by measured
408 peak area for the isotopically labeled internal standard), and blue line is the concentration-weighted
409 (1/x) second-order polynomial fit.

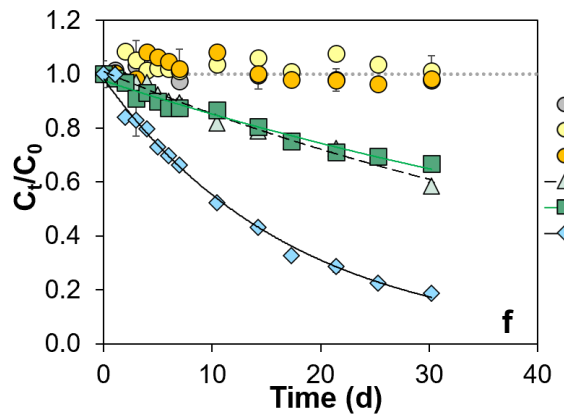
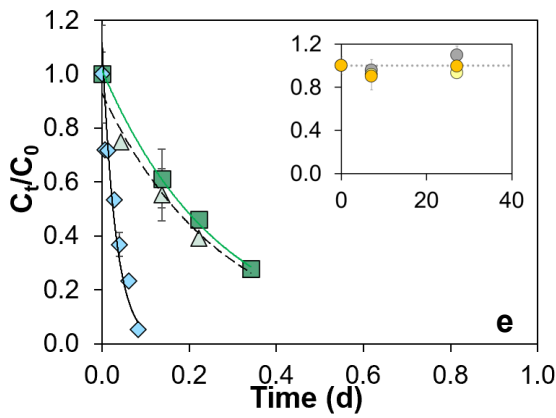
410



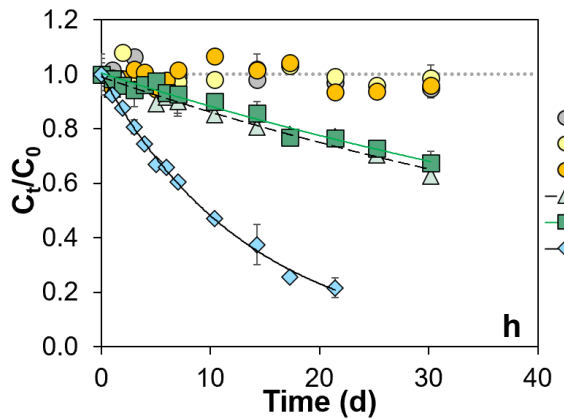
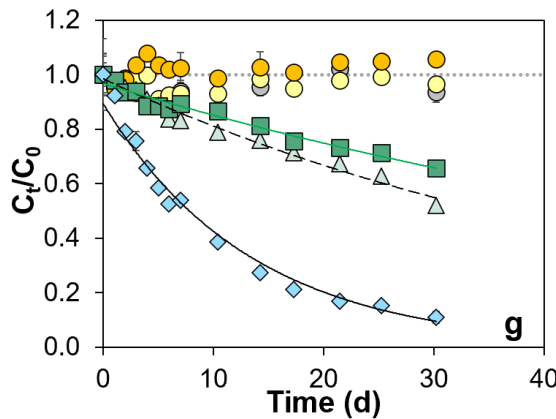
411



412



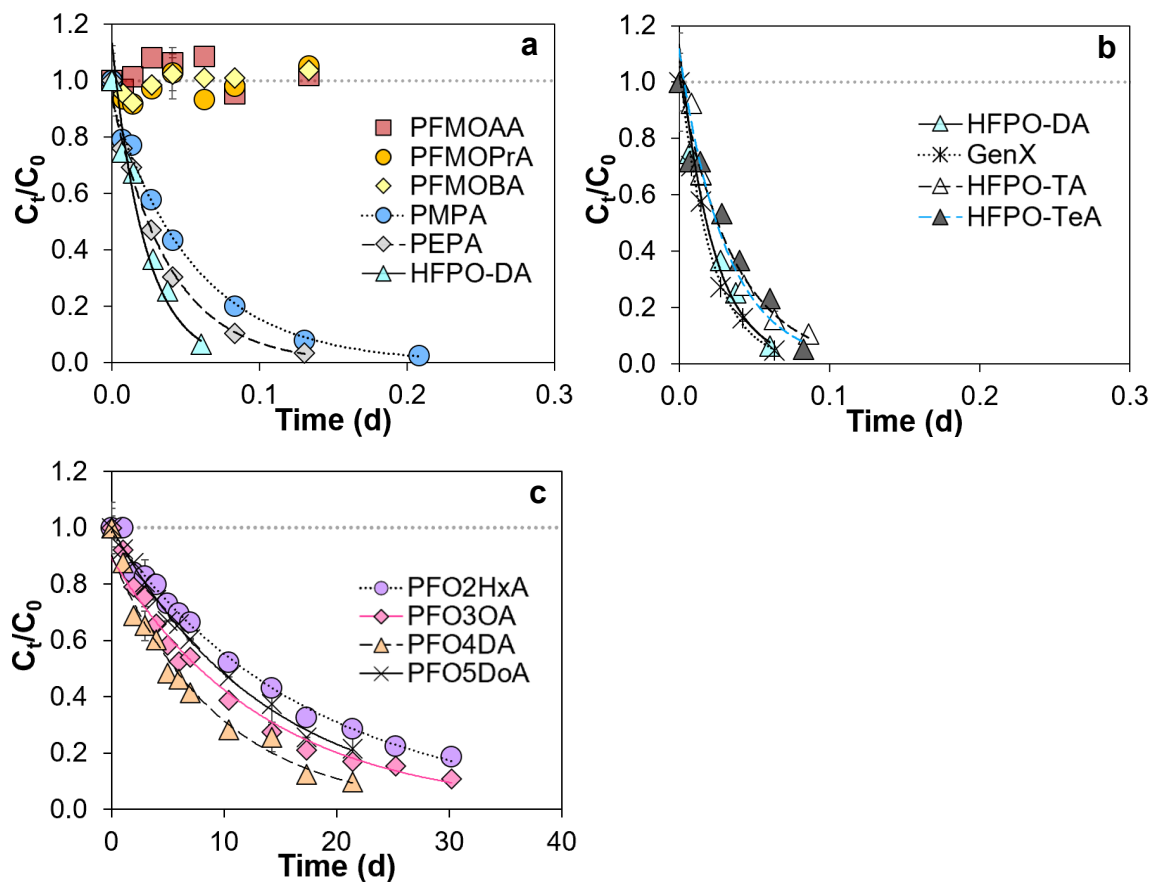
413



414

415 **Figure S3. Stability of (a) PMPA, (b) PEPA, (c) GenX, (d) HFPO-TA, (e) HFPO-TeA, (f)**
416 **PFO2HxA, (g) PFO3OA, and (h) PFO5DoA in water, methanol, isopropyl alcohol (IPA),**
417 **dimethyl sulfoxide (DMSO), acetonitrile (ACN), and acetone at room temperature (20.2°C).**
418 Curves represent first-order kinetic model results, and the corresponding rate constants are given
419 in Table 2. For ease of data comparison, all analyte concentrations were normalized to the initial
420 concentration (C_t/C_0). Error bars represent standard deviations of duplicate measurements. See
421 Figure S1 for compound structures.

422



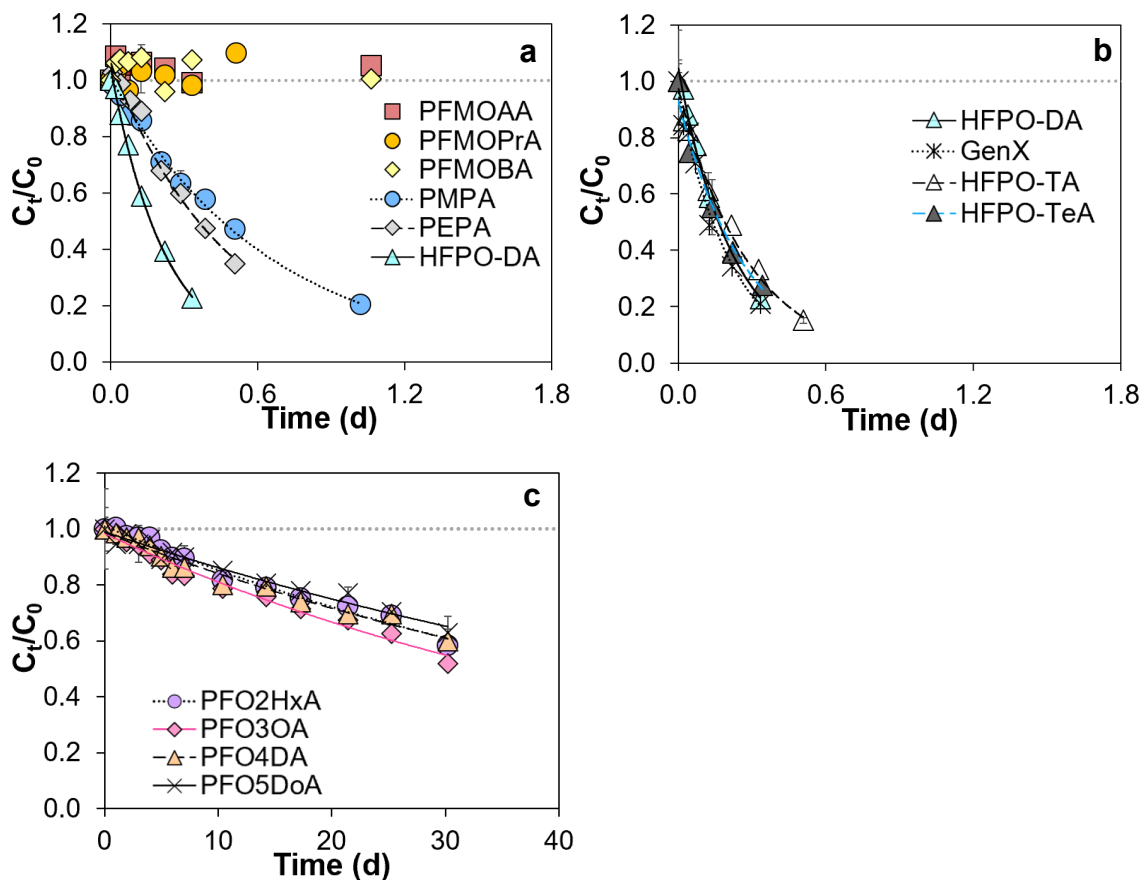
423

424

425 **Figure S4. Stability of perfluoroalkyl ether carboxylic acids (PFECAs): (a) mono-ether**
 426 **PFECAs, (b) HFPO homologues, and (c) multi-ether PFECAs in acetone at room**
 427 **temperature (20.2°C).**

428 Curves represent first-order kinetic model results, and the corresponding rate constants are given
 429 in Table 2. HFPO-DA is plotted in both panel (a) and (b) for comparison. For ease of data
 430 comparison, all analyte concentrations were normalized to the initial concentration (C_t/C_0). Error
 431 bars represent standard deviations of duplicate measurements. See Figure S1 for compound
 432 structures.

433

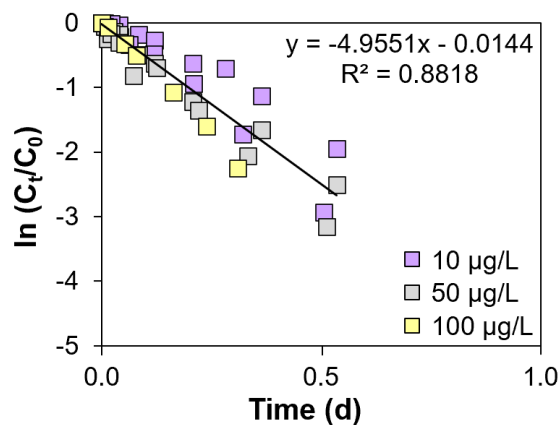


434

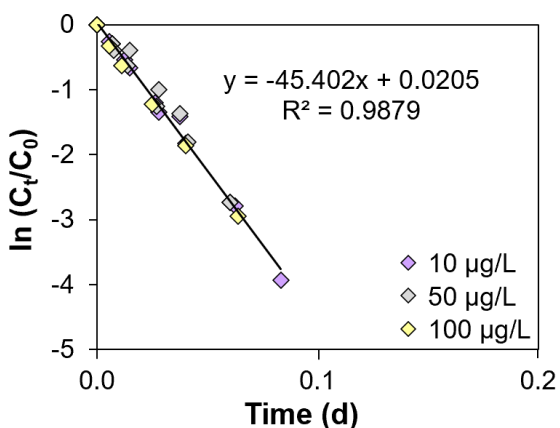
435

436 **Figure S5. Stability of perfluoroalkyl ether carboxylic acids (PFECAs): (a) mono-ether**
 437 **PFECAs, (b) HFPO homologues, and (c) multi-ether PFECAs in dimethyl sulfoxide (DMSO)**
 438 **at room temperature (20.2°C).**

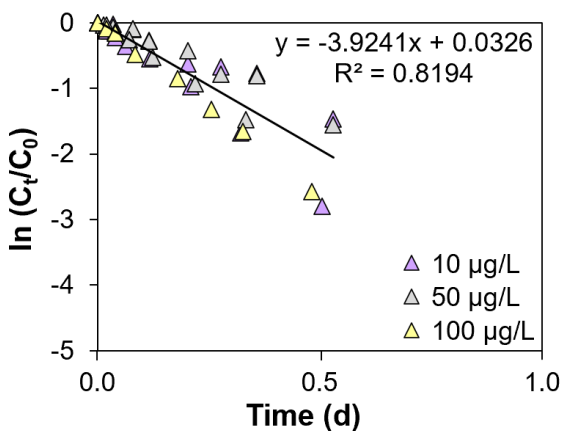
439 Curves represent first-order kinetic model results, and the corresponding rate constants are given
 440 in Table 2. HFPO-DA is plotted in both panel (a) and (b) for comparison. For ease of data
 441 comparison, all analyte concentrations were normalized to the initial concentration (C_t/C_0). Error
 442 bars represent standard deviations of duplicate measurements. See Figure S1 for compound
 443 structures.



444 (a)



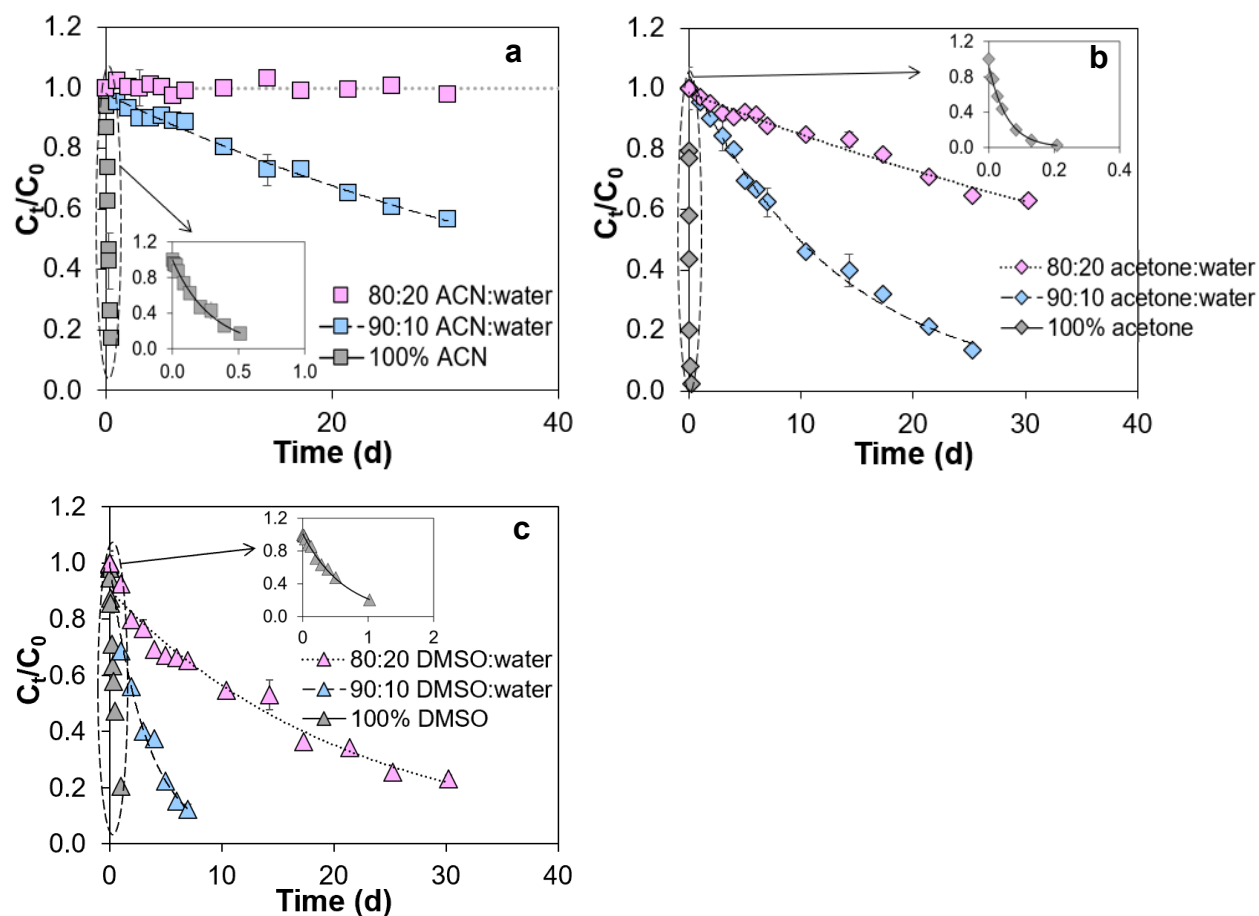
445 (b)



446 (c)

447 **Figure S6. Stability of HFPO-DA starting at different initial concentrations (10, 50 and 100**
 448 **µg/L) in (a) acetonitrile (ACN), (b) acetone, and (c) dimethyl sulfoxide (DMSO) at room**
 449 **temperature (20.2°C).**

450 For ease of data comparison, all analyte concentrations were normalized to the initial concentration
 451 (C_t/C_0). Error bars represent standard deviations of duplicate measurements. See Figure S1 for
 452 compound structures.



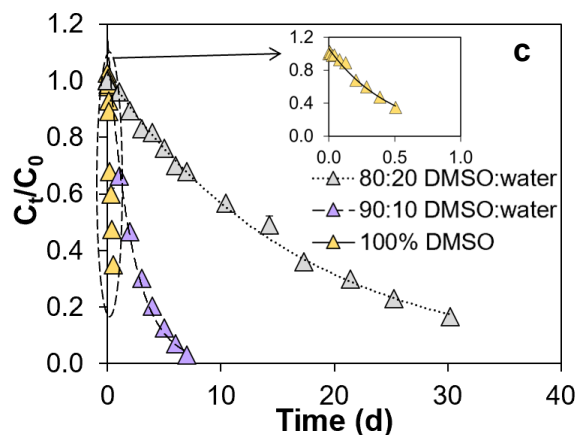
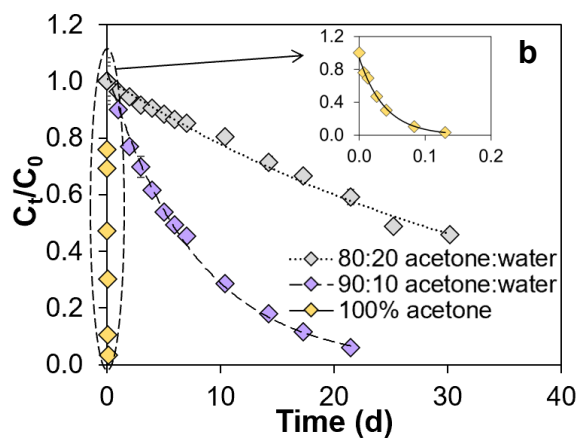
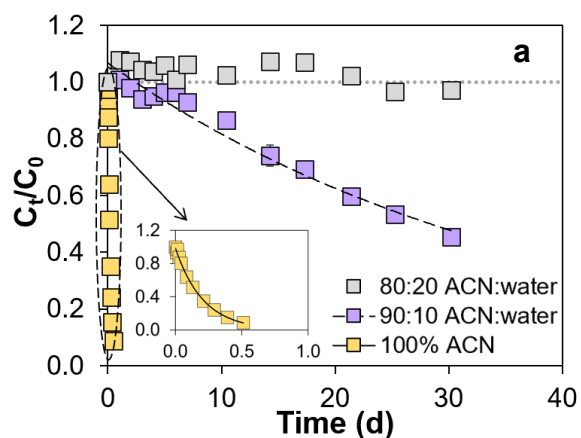
453

454

455 **Figure S7. Stability of PMPA in (a) acetonitrile (ACN), (b) acetone, and (c) dimethyl**
 456 **sulfoxide (DMSO) with different water-to-organic solvent ratios at room temperature**
 457 **(20.2°C).**

458 Curves represent first-order kinetic model results, and the corresponding rate constants are given
 459 in Tables 2 and S9. The inset in each panel highlights results for PMPA in 100% organic solvent.
 460 For ease of data comparison, all analyte concentrations were normalized to the initial concentration
 461 (C_t/C_0). Error bars represent standard deviations of duplicate measurements. See Figure S1 for
 462 compound structures.

463



464

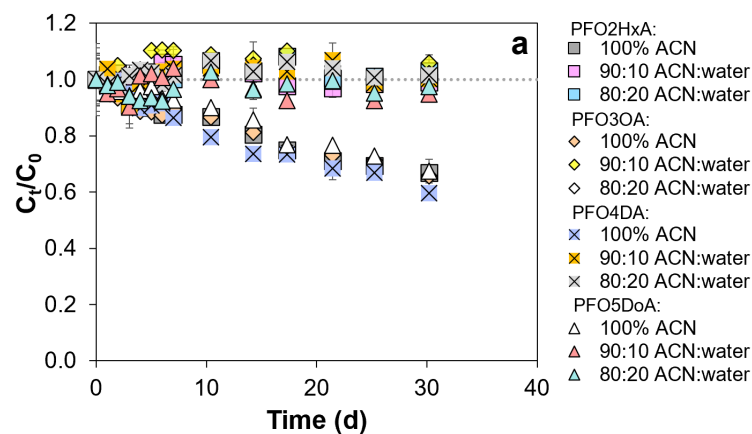
465

466 **Figure S8. Stability of PEPA in (a) acetonitrile (ACN), (b) acetone, and (c) dimethyl sulfoxide**
 467 **(DMSO) with different water-to-organic solvent ratios at room temperature (20.2°C).**

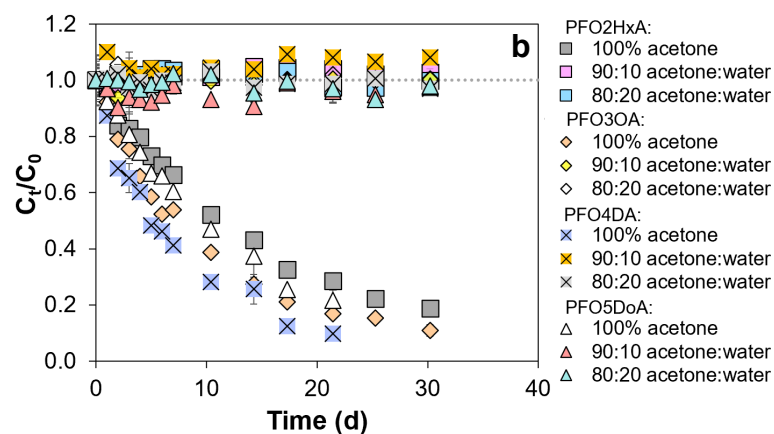
468 Curves represent first-order kinetic model results, and the corresponding rate constants are given
 469 in Tables 2 and S9. The inset in each panel highlights results for PEPA in 100% organic solvent.
 470 For ease of data comparison, all analyte concentrations were normalized to the initial concentration
 471 (C_t/C_0). Error bars represent standard deviations of duplicate measurements. See Figure S1 for
 472 compound structures.

473

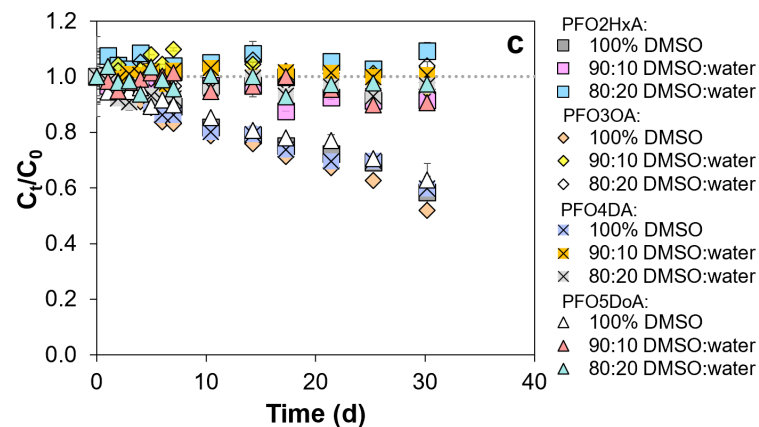
474



475



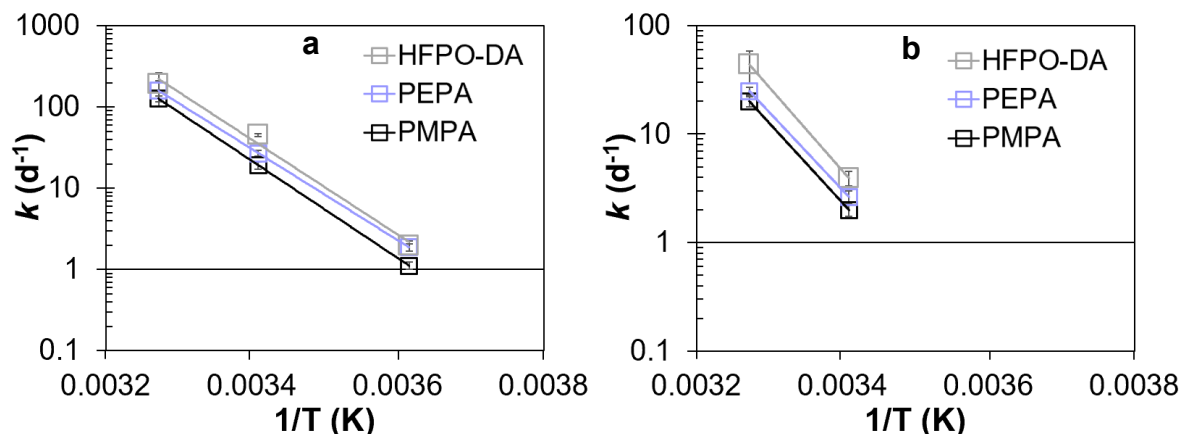
476



477

478 **Figure S9. Stability of multi-ether PFECAs in (a) acetonitrile (ACN), (b) acetone, and (c)**
 479 **dimethyl sulfoxide (DMSO) with different water-to-organic solvent ratios at room**
 480 **temperature (20.2°C).**

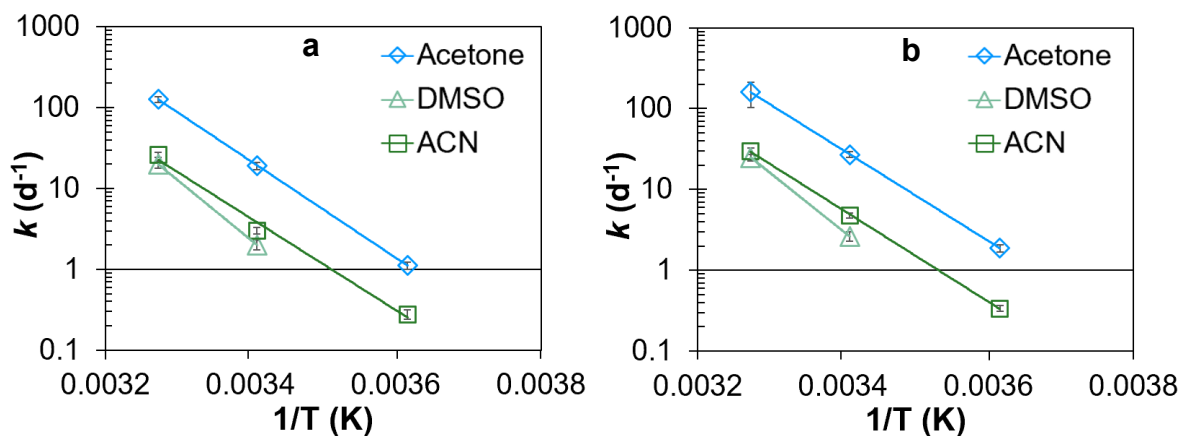
481 For ease of data comparison, all analyte concentrations were normalized to the initial concentration
 482 (C_t/C_0). Error bars represent standard deviations of duplicate measurements. See Figure S1 for
 483 compound structures.



484
 485 **Figure S10. Arrhenius plots describing the temperature-dependence of first-order rate**
 486 **constants of HFPO-DA, PEPA, and PMPA degradation in (a) acetone and (b) dimethyl**
 487 **sulfoxide (DMSO).**

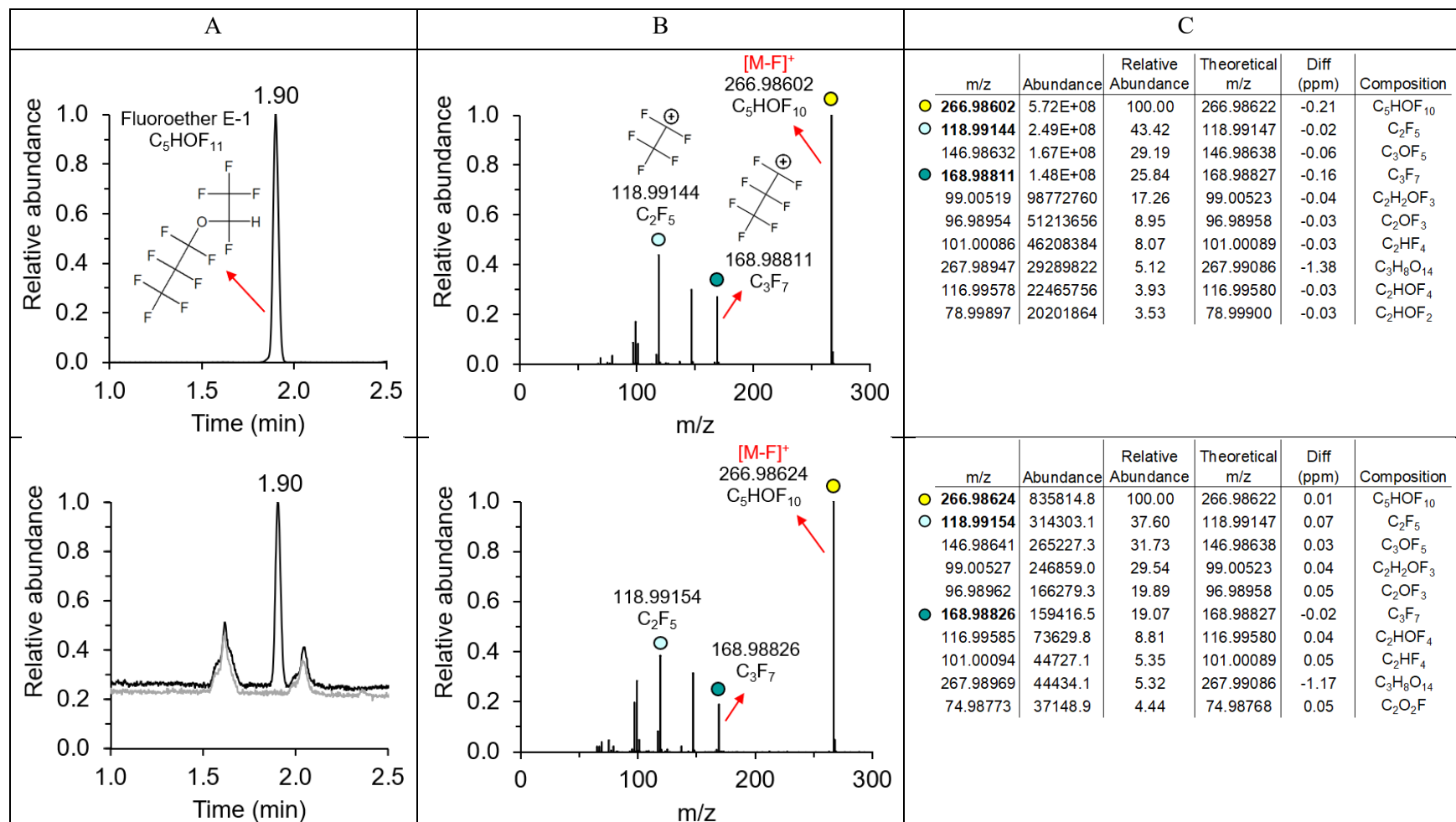
488 The first-order rate constants at different temperatures are given in Table S10. Temperature was
 489 recorded at least four times during the test and average temperature was reported. Experiment was
 490 not conducted at 3.4°C in DMSO due to the high melting point of DMSO (19°C). See Figure S1
 491 for compound structures.

492

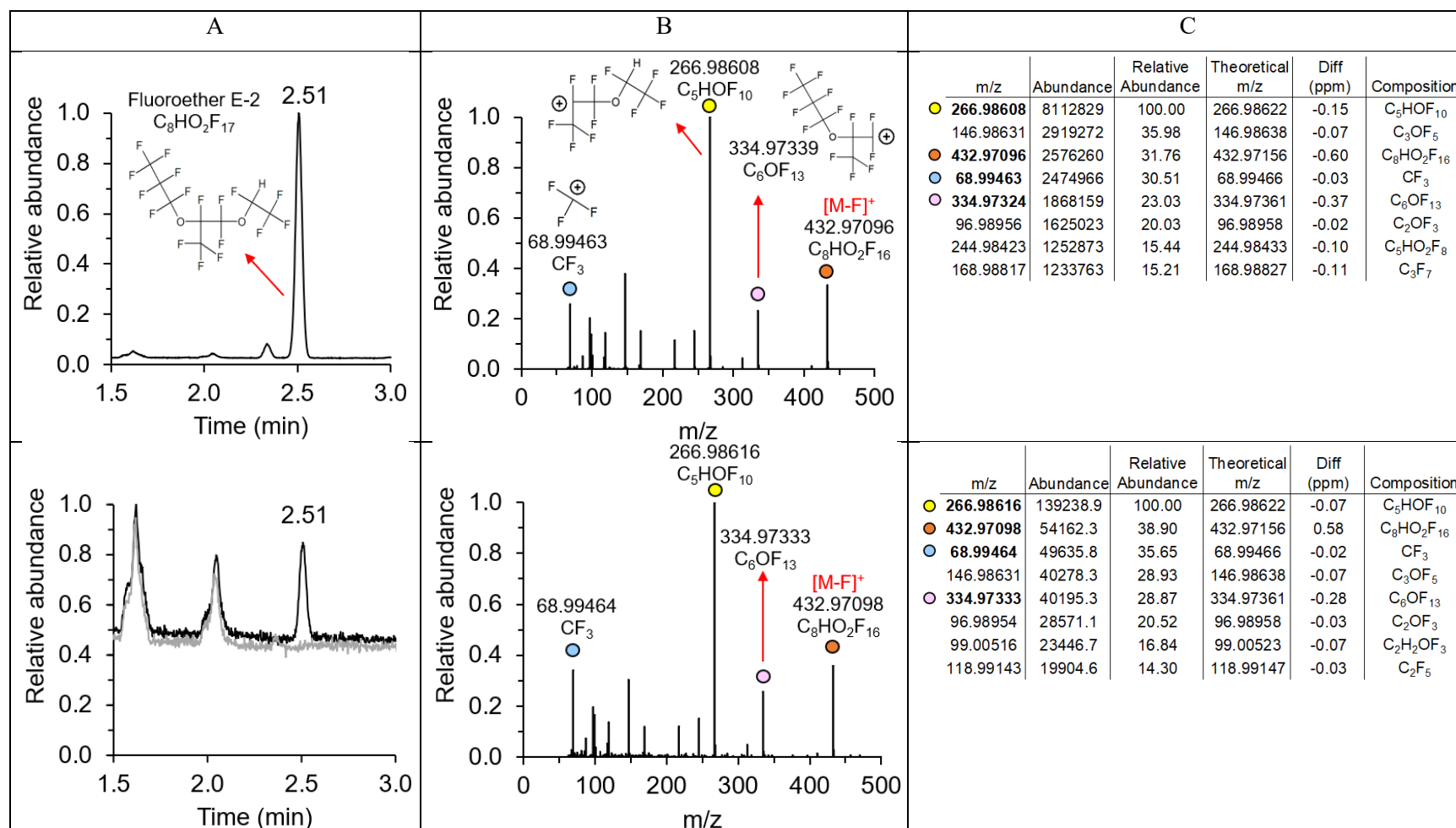


493
 494 **Figure S11. Arrhenius plots describing the temperature-dependence of first-order rate**
 495 **constants of (a) PMPA and (b) PEPA degradation in acetonitrile (ACN), acetone, and**
 496 **dimethyl sulfoxide (DMSO).**

497 The first-order rate constants at different temperatures are given in Table S10. Temperature was
 498 recorded at least four times during the test and average temperature was reported. Experiment was
 499 not conducted at 3.4°C in DMSO due to the high melting point of DMSO (19°C). See Figure S1
 500 for compound structures.

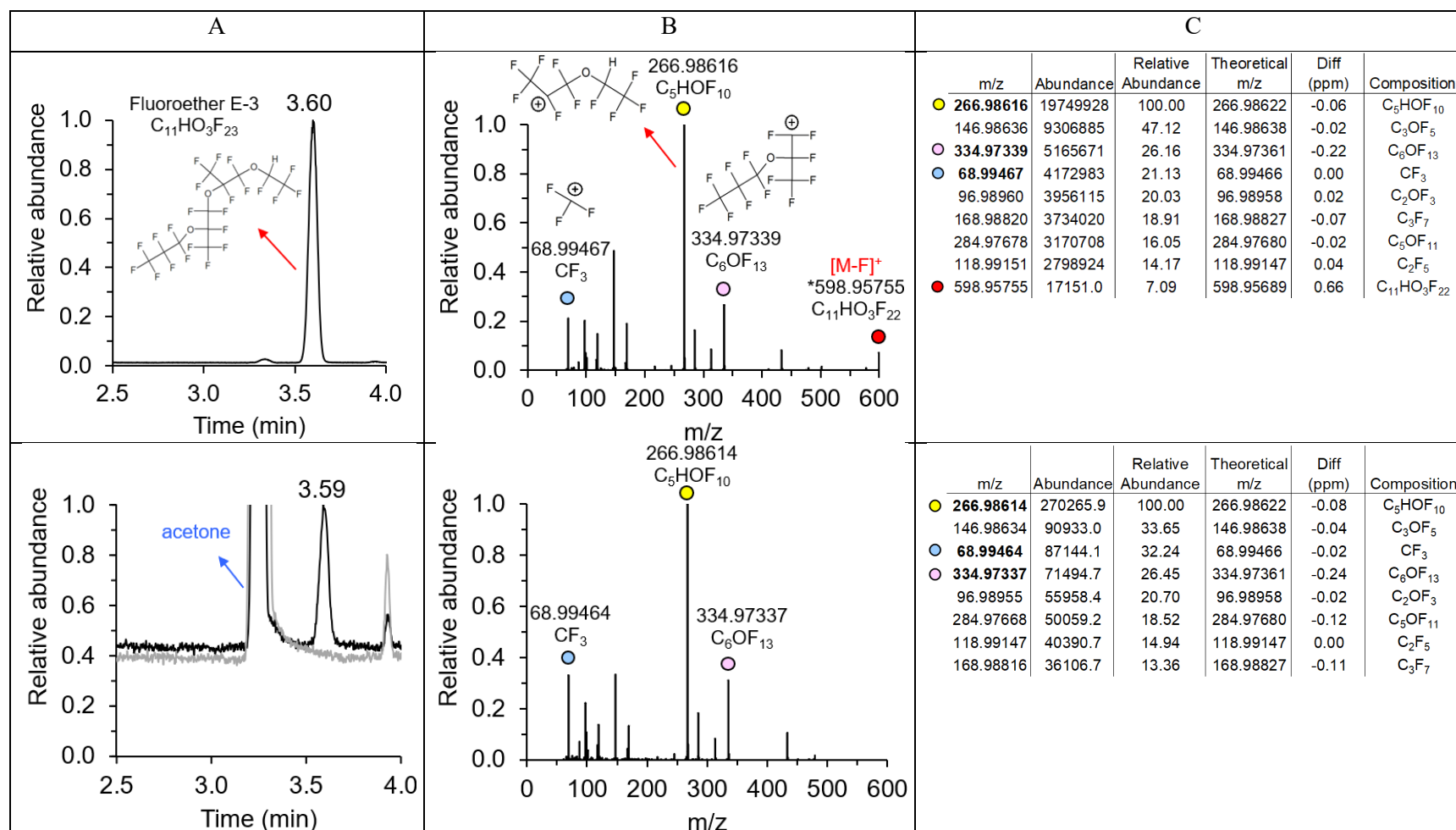


502 **Figure S12. (A) GC-Orbitrap total ion chromatogram (TIC) comparison of Fluoroether E-1 standard (top) and degradation**
 503 **product of HFPO-DA in acetone in 5 days in black color and acetone blank in gray color (bottom); (B) mass spectra of**
 504 **Fluoroether E-1 standard (top) and degradation product of HFPO-DA in acetone in 5 days (bottom); (C) mass spectra list of**
 505 **Fluoroether E-1 standard (top) and degradation product of HFPO-DA in acetone in 5 days (bottom).**



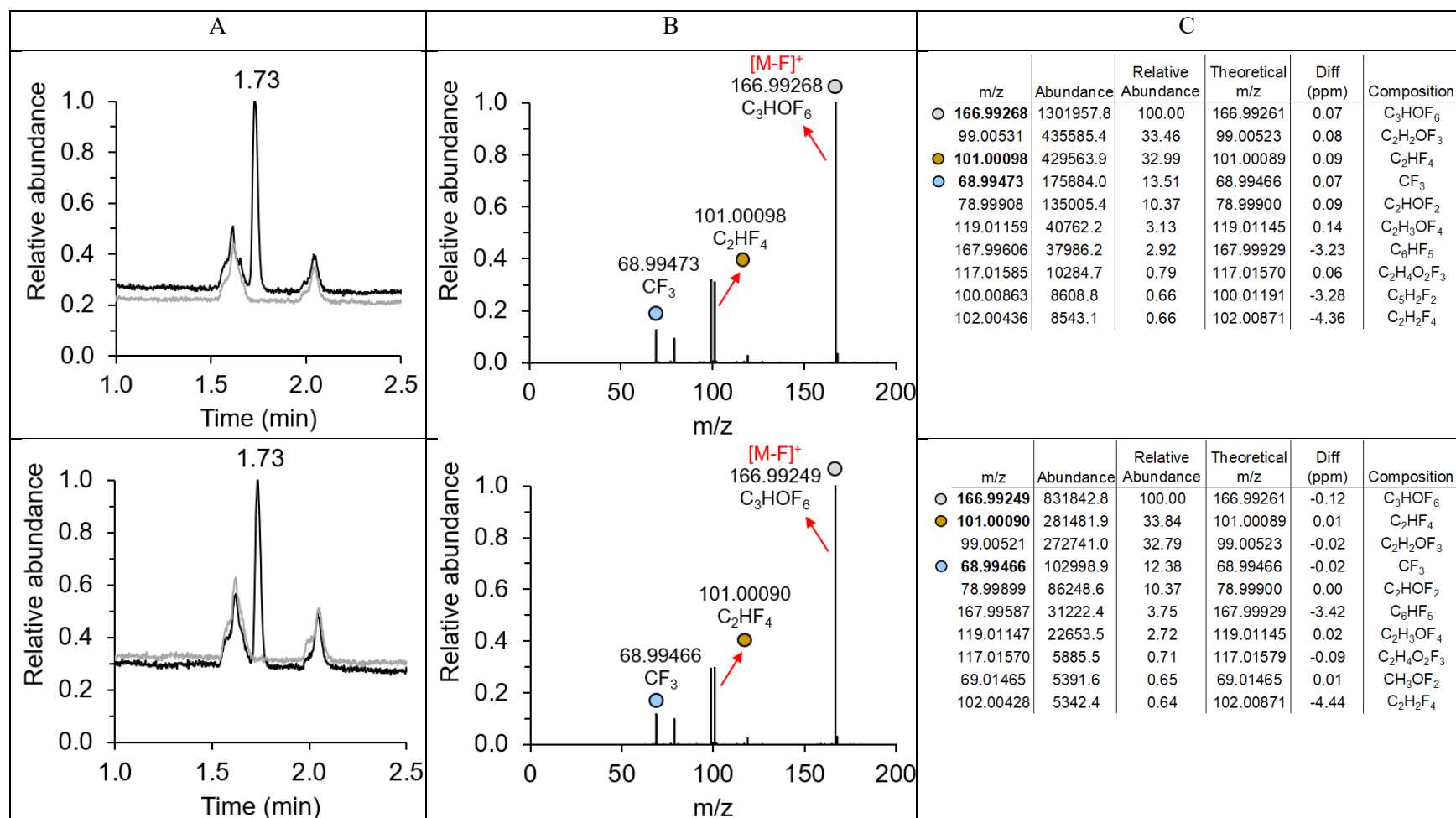
506 **Figure S13. (A) GC-Orbitrap total ion chromatogram (TIC) comparison of Fluoroether E-2 standard (top) and degradation**
 507 **product of HFPO-TA in acetone in 5 days in black color and acetone blank in gray color (bottom); (B) mass spectra of**
 508 **Fluoroether E-2 standard (top) and degradation product of HFPO-TA in acetone in 5 days (bottom); (C) mass spectra list of**
 509 **Fluoroether E-2 standard (top) and degradation product of HFPO-TA in acetone in 5 days (bottom).**

510

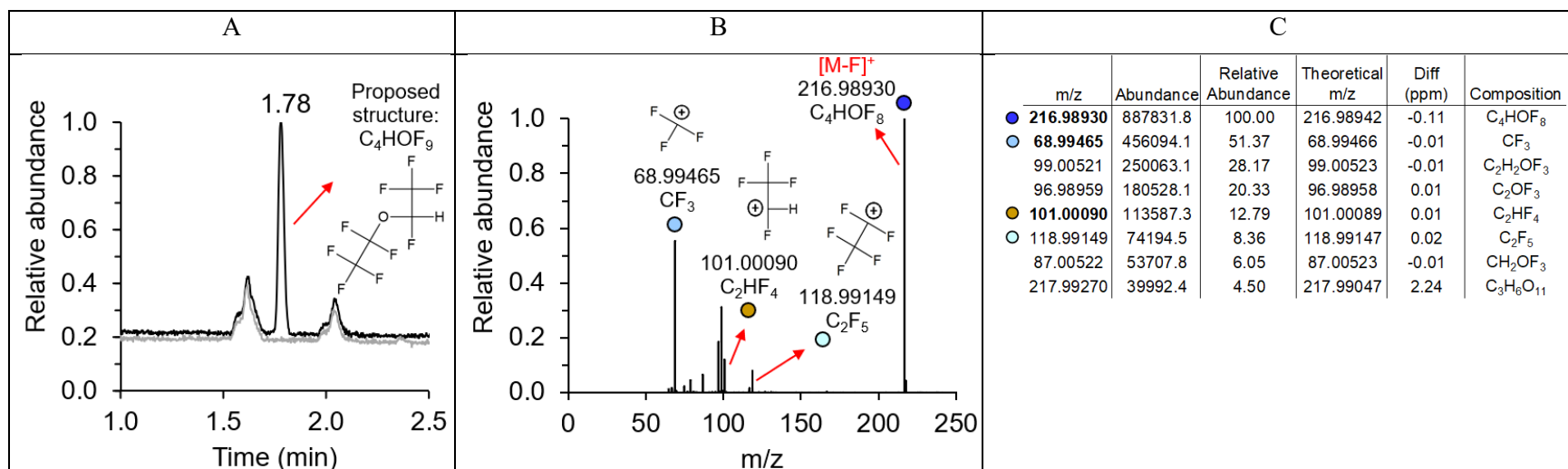


511 **Figure S14. (A) GC-Orbitrap total ion chromatogram (TIC) comparison of Fluoroether E-3 standard (top) and degradation**
 512 **product of HFPO-TeA in acetone in 5 days in black color and acetone blank in gray color (bottom); (B) mass spectra of**
 513 **Fluoroether E-3 standard (top) and degradation product of HFPO-TeA in acetone in 5 days (bottom); (C) mass spectra list of**
 514 **Fluoroether E-3 standard (top) and degradation product of HFPO-TeA in acetone in 5 days (bottom).**

515 *m/z = 598.95755 was only observed in Fluoroether E-3 standard due to its relatively high abundance.

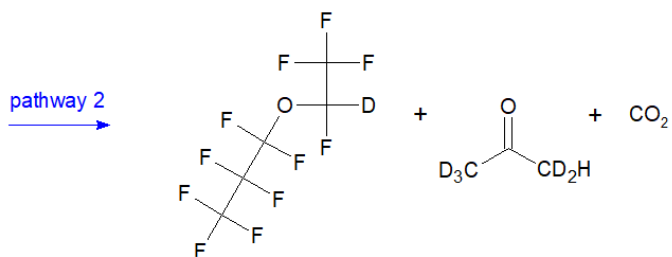
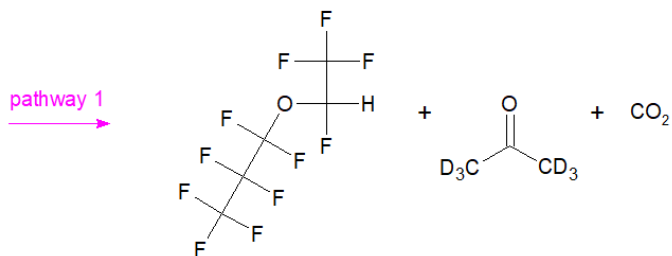
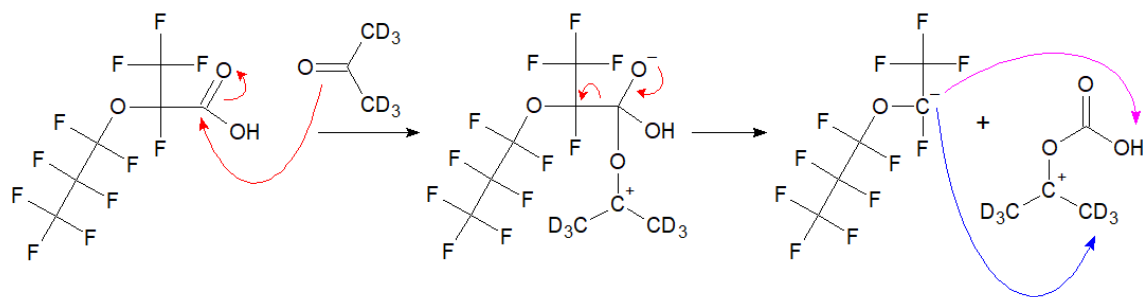


516 **Figure S15. (A) GC–Orbitrap total ion chromatogram (TIC) comparison of degradation product of PMPA in acetonitrile in 5**
 517 **days (top) and degradation product of PMPA in DMSO in 5 days (bottom); (B) mass spectra of degradation product of PMPA**
 518 **in acetonitrile in 5 days (top) and degradation product of PMPA in DMSO in 5 days (bottom); (C) mass spectra list of**
 519 **degradation product of PMPA in acetonitrile in 5 days (top) and degradation product of PMPA in DMSO in 5 days (bottom).**
 520 Solvent blanks are depicted in gray color in (A).



521 **Figure S16. (A) GC–Orbitrap total ion chromatogram (TIC) of degradation product of PEPA in acetone in 5 days in black color**
 522 **and acetone blank in gray color; (B) mass spectra of degradation product of PEPA in acetone in 5 days; (C) mass spectra list of**
 523 **degradation product of PEPA in acetone in 5 days.**

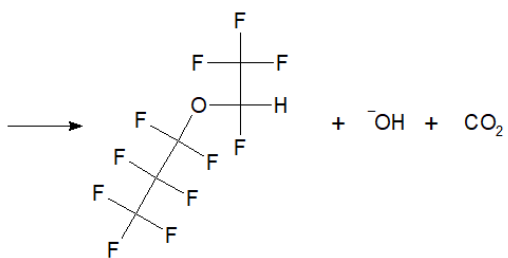
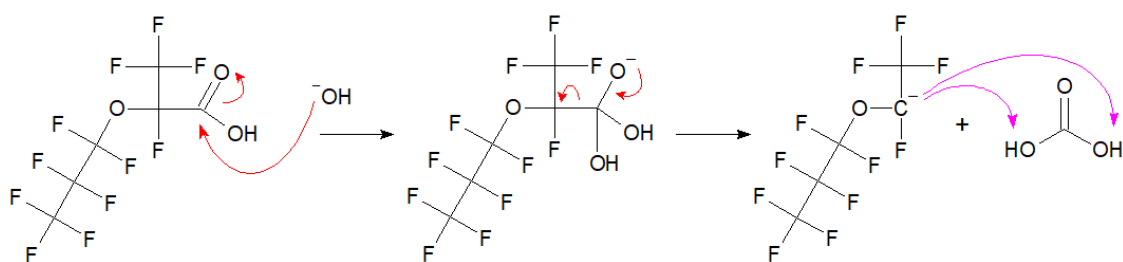
524 **Scheme 1**



525

526

527 **Scheme 2**

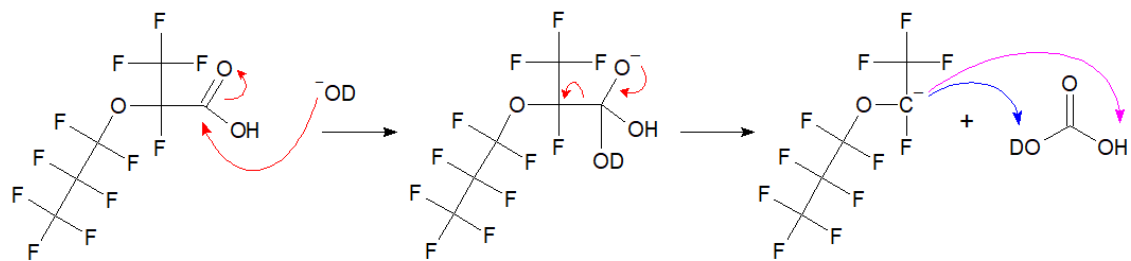


528

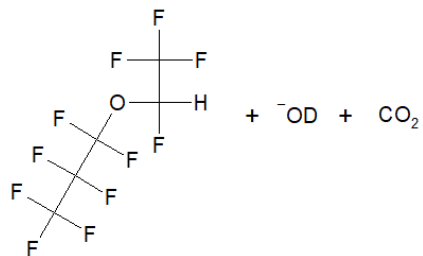
529

530

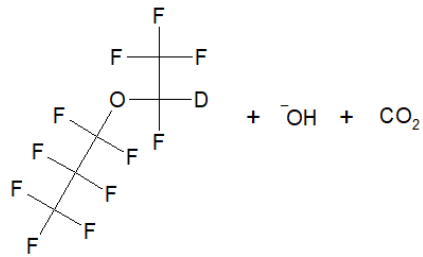
531 **Scheme 3**



pathway 1



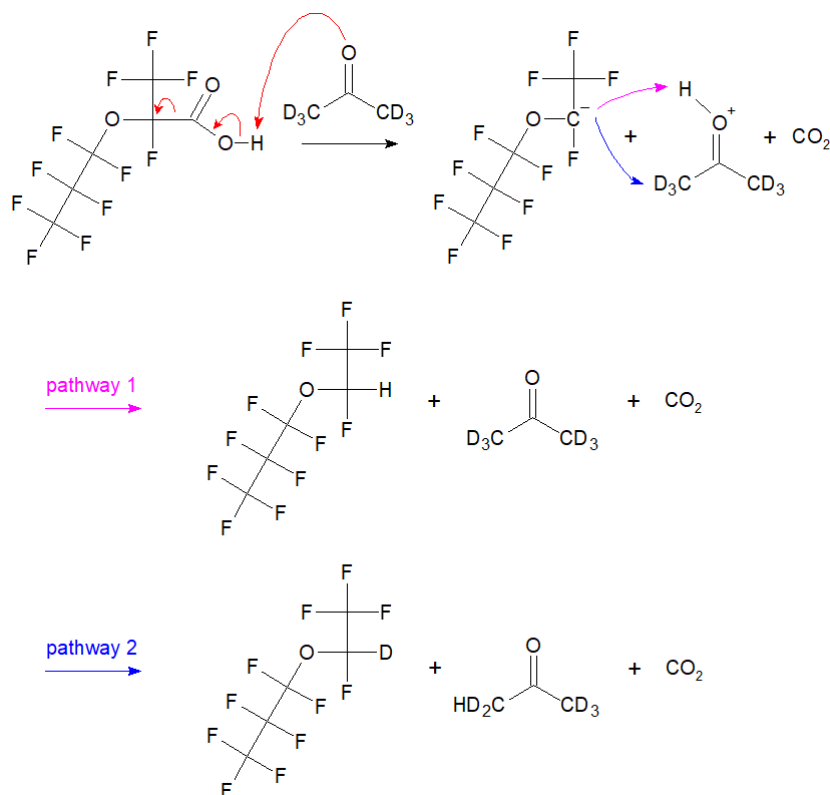
pathway 2



532

533

534 **Scheme 4 [proposed in Liberatore et al. (2020)⁴]**



537 **Figure S17. Proposed mechanisms of HFPO-DA degradation of Fluoroether E-1 in**
538 **deuterated acetone.**

539 Note: arrow shows the direction of electron attack.

540

541 **References**

- 542 (1) McCord, J.; Strynar, M. Identification of Per- and Polyfluoroalkyl Substances in the Cape
543 Fear River by High Resolution Mass Spectrometry and Nontargeted Screening. *Environ.*
544 *Sci. Technol.* **2019**, *53*, 4717–4727.
- 545 (2) Hopkins, Z. R.; Sun, M.; DeWitt, J. C.; Knappe, D. R. U. Recently Detected Drinking
546 Water Contaminants: GenX and Other Per- and Polyfluoroalkyl Ether Acids. *J. Am. Water*
547 *Works Assoc.* **2018**, *110* (7), 13–28. <https://doi.org/10.1002/awwa.1073>.
- 548 (3) Zhang, C.; Hopkins, Z. R.; McCord, J.; Strynar, M. J.; Knappe, D. R. U. Fate of Per- And
549 Polyfluoroalkyl Ether Acids in the Total Oxidizable Precursor Assay and Implications for
550 the Analysis of Impacted Water. *Environ. Sci. Technol. Lett.* **2019**, *6* (11), 662–668.
- 551 (4) Liberatore, H. K.; Jackson, S. R.; Strynar, M. J.; Mccord, J. P. Solvent Suitability for
552 HFPO-DA (“ GenX ” Parent Acid) in Toxicological Studies. *Environ. Sci. Technol. Lett*
553 **2020**, *7*, 477–481.
- 554 (5) Sun, M.; Arevalo, E.; Strynar, M.; Lindstrom, A.; Richardson, M.; Kearns, B.; Pickett, A.;
555 Smith, C.; Knappe, D. R. U. Legacy and Emerging Perfluoroalkyl Substances Are
556 Important Drinking Water Contaminants in the Cape Fear River Watershed of North
557 Carolina. *Environ. Sci. Technol. Lett.* **2016**, *3* (12), 415–419.
- 558 (6) Strynar, M.; Dagnino, S.; McMahan, R.; Liang, S.; Lindstrom, A.; Andersen, E.;
559 McMillan, L.; Thurman, M.; Ferrer, I.; Ball, C. Identification of Novel Perfluoroalkyl
560 Ether Carboxylic Acids (PFECAs) and Sulfonic Acids (PFESAs) in Natural Waters Using
561 Accurate Mass Time-of-Flight Mass Spectrometry (TOFMS). *Environ. Sci. Technol.*
562 **2015**, *49* (19), 11622–11630.
- 563